Thomas Brunner

Analysis of indicators for the assessment of drowsiness of truck drivers

Diploma thesis

Institute of Medical Engineering
Graz University of Technology
Kronesgasse 5/II, A-8010 Graz
Head: Univ.-Prof. DI. Dr. Rudolf Stollberger

Supervisor: Ao.Univ.-Prof. DI. Dr. Hermann Scharfetter

Evaluator: Ao.Univ.-Prof. DI. Dr. Hermann Scharfetter

Graz, July 2011

EIDESSTATTLICHE ERKLÄRUNG

Ich erkläre an Eides statt, dass ich die vorliegende Arbeit selbstständig verfasst, andere als die angegebenen Quellen/Hilfsmittel nicht benutzt, und die den benutzten Quellen wörtlich und inhaltlich entnommene Stellen als solche kenntlich gemacht habe.

Graz, am _____ _____

Datum Unterschrift

STATUTORY DECLARATION

I declare that I have authored this thesis independently, that I have not used other than the declared sources / resources, and that I have explicitly marked all material which has been quoted either literally or by content from the used sources.

Graz, _____ _____

Date Signature

Acknowledgments

I would like to thank the Virtual Vehicle Competence Center for the opportunity to realize this diploma thesis. Furthermore I would like to thank all people from the Area D for their support and friendliness.

Also, I would like to express my gratitude to my supervisor from the Technical University of Graz, Dr. Hermann Scharfetter and to my supervisor from the Virtual Vehicle, DI Wolfgang Tengg for their expertise and assistance during the development of this work.

Finally, I would like to thank my whole family, especially my parents for the support they provided me through my entire life.

Analyse von Messgrößen zur Müdigkeits-Beurteilung von LKW-Fahrern

Erhöhte Müdigkeit im Straßenverkehr, insbesondere bei Nutzfahrzeuglenkern, ist ein hoher Risikofaktor, welcher zu gefährlichen Situationen und Unfällen führen kann. Um den LKW-Arbeitsplatz des Berufskraftfahrers hinsichtlich möglichst geringen Müdigkeitspotentials zu entwickeln und herzustellen, ist die Analyse von Müdigkeitszuständen des Fahrers notwendig.

Hierfür wurde eine direkte Methode, welche physiologische Signale des Fahrers zur Müdigkeitserkennung benutzt, sowie eine indirekte Methode, welche den Aufmerksamkeitsgrad des Fahrers durch Fahrzeugparameter abbildet, angewandt.Als direkte Methode wurde die Herzratenvariabilität (HRV), und als indirekte Methode der Lenkwinkelverlauf verwendet. Bei Messfahrten wurde neben der Aufzeichnung der Daten der beiden Methoden, auch eine subjektive Müdigkeitsbewertung des Fahrers angegeben. Zusätzlich wurden 12 Probanden einer Studie zur Reaktionszeit-Ermittlung bei Schlafentzug unterzogen, um die Müdigkeitsanalyse aus der HRV zu validieren.

Bei der Auswertung der Daten der Messfahrt, zeigte eine subjektiv angegebene Müdigkeit, nur teilweise einen Zusammenhang mit der HRV, der Lenkwinkel jedoch zeigte stets einen dementsprechenden Verlauf. Aus der Reaktionszeit-Studie wurde eine Gruppierung, in Personen bei welchen sich die Müdigkeit in der HRV abzeichnet, und in Personen bei denen das nicht der Fall ist, durchgeführt.

Da auch Faktoren, wie Langeweile oder Ablenkung, Einfluss auf die Veränderung des Lenkverhaltens haben können, ist eine Beurteilung der Müdigkeit aus dem Lenkwinkel keine vollkommen zuverlässige Methode. Um die Müdigkeit aus der HRV zu erkennen, müssen zukünftige Probanden einer Voruntersuchung unterzogen werden, aus welcher nur Personen mit HRV-Ansprechverhalten infolge von Müdigkeit zu Messfahrten herangezogen werden können.

Schlagwörter: LKW, Müdigkeit, Herzratenvariabilität, Lenkwinkel, Cluster-Analyse

Analysis of indicators for the assessment of drowsiness of truck drivers

Increased drowsiness in traffic, especially in professional truck drivers, is a major risk factor, which can lead to dangerous situations and accidents. To develop and produce the truck driver´s workplace, in a way to minimize the stimulation of drowsiness on the driver, the analysis of drowsiness phases of the driver is crucial.
Therefore a direct method, which uses physiological signals from the driver to monitor the drowsiness level, and a indirect method, which detects the attention level through vehicle parameters, was applied. For the direct method the heart rate variability (HRV) and for the indirect method the steering angle progression was used. At test rides, besides logging the data of these two methods, a subjective drowsiness rating from the driver was denoted. Additionally 12 subjects attended at a study to determine the reaction time during sleep deprivation, in order to validate the analysis of drowsiness through the HRV.
The analysis of the test rides revealed, that the HRV showed did not always show a relation with the subjective drowsiness rating, in contrast to the steering angle, which always showed a correlating progression. A cluster analysis was performed in order to identify people who show high correlation between HRV and drowsiness and people who do not show this correlation.
The fact that factors, like boredom or distraction, can also have an influence on the steering behavior, the assessment of drowsiness through the steering angle is not an entirely reliable method. For detecting drowsiness from the HRV, future subjects have to attend a pre-examination, from which only people with a HRV response to drowsiness should be recruited for further test rides.

Keywords: Truck, Drowsiness, Heart rate variability, Steering angle, Cluster-analysis

Contents

List of Abbreviations

ECG	Electrocardiography
EEG	Electroencephalography
FFT	Fast fourier transform
HRV	Heart rate variability
MWSA	Mayer-wave related sinus arrhythmia
PERCLOS	Percentage of eye closure
pNN50	Percentage of pairs of RR Intervals differing more than 50ms
RMSSD	Root mean square of differences between adjacent RR-Intervals
RSA	Respiratory sinus arrythmia
RT	Reaction time
SDRR	Standard deviation of RR Intervals
SIT	Steering interval time
SRR	Steering wheel reversal rate
SSS	Stanford sleepiness scale
STFT	Short time fourier transform

1 Introduction

Professional drivers in the commercial transport system have an increased risk for decreased attention and increased drowsiness during their work. Many and irregular working hours, long driving time, time pressure, inadequate recovery, bad sleep quality, driving at night, shift work and monotonous road conditions are typical factors for establishing inattention and fatigue. According to a study from [1], fatigue, after excessive speed, was indicated as the second most cause of accidents. In 19% of all accidents involving a truck with an overall weight of more than 7.5 tons, fatigue was the main reason for the accident. From accidents during nightdriving 42%, and from accidents between 14am and 17am, 11% were attributed to fatigue.

The commercial transport of goods is a fundamental element in the economic system. In Austria the biggest part of this transportation is done with trucks with a transport capacity of 29,1 Mrd. tonskilometer, exceeding the railway transportion with 17,8 Mrd. tonskilometer[1]. In comparison to a normal car driver, who, under normal circumstances, can decide how long he drives, a professional truck driver, as regulated by the law, has to drive up to ten hours per day. So the truck is the working place for the truck driver and has to be designed for optimal safety and comfort. Time pressure and monotonous work is especially a factor in long distance truck driving and can lead to exhaustion of the driver. Subsequently rising exhaustion can result in drowsiness, and in the worst case in microsleeps. Keeping in mind that a fully loaded truck trailer has a weight of up to 40 tons, it is clear that a drowsy driver is a dangerous factor on public roads. Changing the boundary conditions in a truck driver´s workday will not happen that easy, due to competition and time pressure, so the truck manufacturers have to design there vehicles in the best way to keep the driver fit and safe.

To start with this assignment it is necessary to analyze the central component of controlling the truck, the human driver. For this purpose an supervised driving study with two subjects for a period of eight days was realized. The aim was to identify and analyze decreased attention levels of the driver and also to find a relationship between the decreased attention level and the behaviour of driving the truck.

[1]Taken from Statistik Austria - http://www.statistik.at

In order to measure the amount of drowsiness a driver can develop during long truck driving work, two basic approaches exist. One is the direct approach, which uses physiological signals from the driver to monitor his alertness level. The other approach is the indirect one, where the operation of the vehicle, resulting from the drivers actions, is analyzed. To make a useful statement, whether the truck makes the driver drowsy, it is necessary to compare the direct with the indirect approach. The direct approach used in this study was the monitoring of the heart, more precisely the measurement of the heart rate variability (HRV). The reason for this decision is the easy use of an electrocardiogram (ECG) monitor, compared to other systems. The steering wheel movements were taken as indirect approach, due the fact that the handling of the steering wheel is the pivotal factor during driving. The pedal operation was excluded, because most truck drivers use the automated speed control instead of operating the accelerator pedal themselves. For obtaining an auxiliary material the two drivers underwent a subjective drowsiness rating every half hour during the driving. The tool, used for the subjective drowsiness rating, was the Stanford sleepiness scale (SSS), which has 8 level ratings of drowsiness with an according number.

In addition, a study named "Reaction time determination under sleep deprivation" was realized. In contrast to the the small number of two subjects in the driving study, this reaction analysis was executed with a bigger number of subjects. The 12 subjects in this study were connected to an ECG monitor and did a reaction test every 30 minutes, which is used for the medical-physiological certificate, which is necessary for getting a class D[2] driving license. They also rated there drowsiness level every 30 minutes according to the Stanford sleepiness scale.

1.1 Purpose of this work

The goal of this diploma thesis is the analysis and interpretation of the measured data from the test rides. Furthermore, evidence for a correlation between the direct and indirect approach for drowsiness detection should be established, in this case, between the heart rate variability and the steering angle. This putative correlation should lead to a conclusion, whether the

[2]Vehicles with a transport capacitivity of more than eight people.

tested truck tends to make the driver drowsy or not. The adequacy of the HRV for measuring the drowsiness should be assessed by comparing different analysing methods and parameters of the HRV. Also different methods of analyzing the steering wheel movements for predicting drowsiness have to be compared. The subjective ratings of drowsiness should support the assessment of analyzing methods based on the HRV and the steering signal. Also the results of the reaction time analysis study have to be compared to these analyzing methods. Finally a correlation between the HRV and the steering wheel movements should be proven.

Based on limited resources, especially time and project staff, less test rides than previously planned could be realized. Also the fact that just one truck was used in the test rides, prevented the comparison between different trucks. Now with this starting position, the analyzing task depends on noticable changes in the measured data, which should lead to an useful predication about the fatigue of each driver. To make an appropriate statement, whether the analysis and the correlation of the measured data are meaningful, a case determination of the 2 drivers is needed.

The findings in the "Reaction time determination during sleep deprivation" study should serve for two statements. The main and important question is, whether the heart rate variability is a meaningful method for indicating fatigue. And on the other hand it is possible to make a self-contained statement, if the reaction time changes with increasing fatigue.

In summary, the main parts of this work are the fatigue analysis of the two drivers, which were included in the truck driving study. The results of the reaction time study should reveal, if it is possible, to detect increased drowsiness with heart rate variability indices. After applying these conclusions to the measured data of the two test drivers, an informative statement should be given, on the possibility of the assessment of drowsiness of truck drivers.

1.2 Heart Rate Variability

Altough the respiratory sinus arrythmia (RSA), as starting point for heart rate analysis, was already discovered in 1733, the appearance of high-resultion heart-monitor devices in the last decade was neccessary to measure subtle heart rate fluctuations [2]. Nowadays its known that the RSA, which reflects the change in heart rate due to inspiration and expiration, and the HRV are related and both reflect vagal cardiac influence. HRV has been of interest in many studies to show a connection to neurological diseases (e.g brainstem cerebral infarctions, brainstem injury, parkinsons disease, multiple sclerosis)[2] and to workload on the living system (e.g autonomic activities, monotonous work)[3].

1.2.1 Fundamentals of HRV

The Heart Rate Variability, as described by the "Task Force of the European Society of Cardiology and the North American Society of Pacing Electrophysiology" [4], denotes the variation in time between two consecutive heart beats. Furthermore HRV is the instantaneous measure of consecutive heart rates as well. So the HRV equates to the oscillations in the interval of consecutive heart beats and heart rates, not in the heart rate itself. The beat to beat interval varies, depending on physiological mechanisms, in a range of about 10-30%, even if the heart rate remains constant [3]. To get a better understanding, where the oscillations in the heart rate are coming, it is necessary to explain the physiological background of the cardiovascular function. This explanation is done in chapter 1.2.4.

To log the continuous heart beats, it is necessary to extract the R-peaks from an electrocardiogram. The basics and the origin of the electrocardiogram are described in the following chapter.

1.2.2 Origin of the electrocardiogram

The rhythmical contraction and relaxation of the artia and the ventricels in the heart are the most essential events in a cardiac cycle. The basis for this rhythmical cycle are the

excitable myocardial cells and their feature of establishing an electrical potential along the cell-membran. This potential is about$-90mV$ at rest and caused, due the permeability of the myocard-cellmembrane for particular ion types. The resting membrane potential can be approximated by the Nernst Equation(1). [5]

$$E = \frac{R \cdot T}{z \cdot F} \cdot ln \frac{c_a}{c_i} \tag{1}$$

Where E is potential on the membrane in mV, R is the gas constant, T the temperature in K,z the ion valency, F the Farady constant and c_a and c_i are the K^+ concentrations outside and inside the membrane.

Normal myocardium cells, like skeletal cells, need an extern impulse to depolarize the membrane above the threshold potential. This exceeding is necessary to initiate an action potential which leads to the cardiac cycle. The myocardium tissue has specialized cells, with a property called automaticity, which reflects an ability to initiate the action potential on their own. Due to this property the autorhythmical activity of the heart is possible. This happens independently of any nerves or hormones, but the intervals between consecutive action potentials are influenced by autonomic nerves. The sympathetic part shortens this interval and leads to higher cycle rates and the parasympathetic part does the opposite. An action potential starts as mentioned above from the resting membrane potential, then it comes to a depolarization, a platea phase and to a repolarization of the myocardium cells. This electrical sequence is initiated from the sinus node and moves along specialized cells in the following order: artrial muscle, AV node, bundle of His, Purkinje fibers and ventricular muscle. During several phases of the propagation of the depolarization wave a resulting electrical potential can be measured on the surface, known as an ECG[6].

For further information about the ECG, please refer to [5, 6].

1.2.3 Analysis of the RR Interval

The electrical events, which are produced by the specialized cells of the conduction system, are too small for tracing with surface electrodes. So the ECG traces essentially the action potentials of the atrial and ventricular muscel cells, from which other events can be deduced. As a consequence, with an ECG, the phases of the cardiac cycle can be described. For a better overview the phases are listed in table 1, taken from [6]:

Physiological Event		ECG Evidence
1.	Sinuatrial node initiates impulse	not visible
2.	Depolarization of artrial muscle	P wave
3.	Artrial connection	not visible
4.	Depolarization of AV node & Common bundle	not visible
5.	Repolarization of ventricular muscle	not visible
6.	Depolarization of ventricular muscle	QRS complex
7.	Contraction of artrial muscle	not visible
8.	Repolarization of ventricular muscle	T wave

Table 1: Events of one cardiac cycle

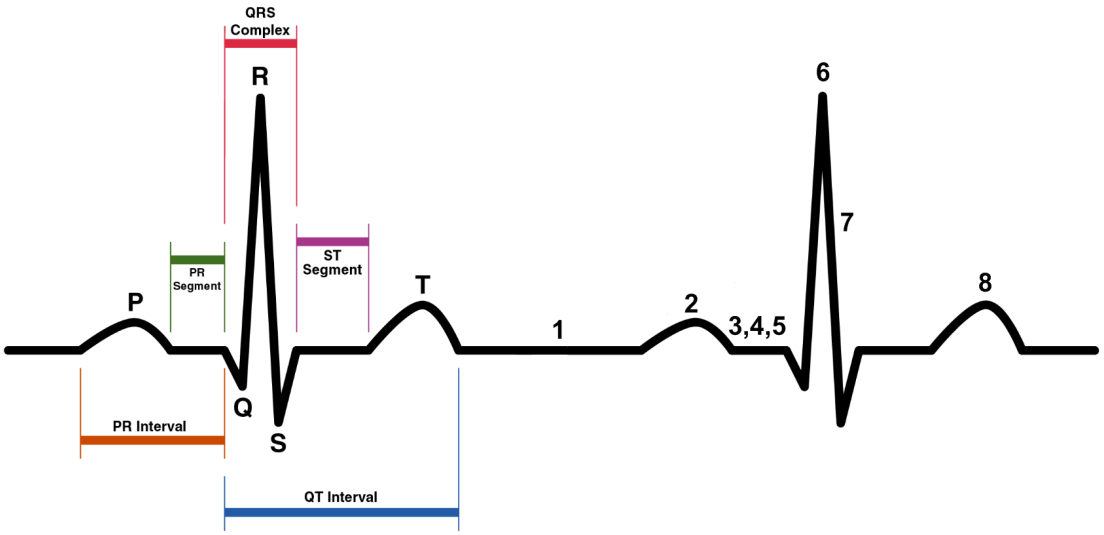

Figure 1: ECG signal of two cardiac cycles

In figure 1 the first cardiac cycle indicates the segments of the ECG signal, the second cardiac cylcle shows the physiological events, which are listed in table 1. Only 3 of the 8 physiological events during one cycle are traced by the ECG measurement[5].

The most important event for HRV Analysis is the QRS complex, especially the R-peak. Now the time interval between two R-peaks is measured, and the continious recording of these intervalls is the source for HRV Analysis.

The R-peak has the biggest amplitude of the QRS complex because the highest potential difference between the intra- and the extracellular membram is present at this point.

A mathematical description for the excitation-process of the myocard cells is the Bidomain Model:

$$I_m = \chi(C_m \frac{\partial V_m}{\partial t} - I_{ion}) \tag{2}$$

Where χ is surface/volume, C_m is the membran capacity, V_m is the potential difference and

I_{ion} is the ion current, the membrane current I_m is:

$$I_m = \nabla \cdot (\sigma_i \nabla \phi_i) = -\nabla \cdot (\sigma_e \nabla \phi_e) \tag{3}$$

Where σ_i and σ_a describing the electrical conductivity in the intra- and the extracellular membram and ϕ_i and ϕ_e the potential of the intra- and the extracellular membram.

1.2.4 Physiological background of cardiovascular function

It would be desirable to have a physiological marker with a direct relationship to the human autonomic activity. Unfortunately the autonomic nervous system is a very complex structure, and so, even after many years of research, a desired marker for drowsiness was not yet been found. Consequently there is an enormous effort of research in this area . There are many proposed markers for indicating autonomic activity, such as heart rate, heart rate variability, heart rate recovery after exercise, baroreflex sensitivity, heart rate turbulence, plasma/coronary sinus catecholamine levels, muscle sympathetic nerve activity and others [7]. Among these parameters the main focus lies on the heart rate measurement, especially the heart rate itself and the heart rate variability, due to the non-invasiveness of the methods and the inexpensive aquisition devices.

The autonomic nervous system and the somatic nervous system are part of the peripheral nervous system. The somatic nervous system consists of nerves that connect the brain and spinal cord with muscles controlled by conscious effort (voluntary or skeletal muscles) and with sensory receptors in the skin [8]. The autonomic nervous system connects the brain stem and spinal cord with internal organs and regulates internal body processes that require no conscious effort. Examples are the rate of heart contractions, blood pressure, the rate of breathing, the amount of stomach acid secreted, and the speed at which food passes through the digestive tract. Furthermore the autonomic nervous system is divided in two parts, the sympathetic part which is peripherally mediated through the transmitter epinephrine and the parasympathetic part, also known as vagal tone, peripherally mediated through the transmitter acetylcholine. As described in chapter 1.2.3 the sinus node is the start area of the polarization

wave which spreads over the whole myocardium afterwards. Due to this effect the pump function of the heart is induced [5]. The activity of the sinus node is influenced by both the sympathetic and parasympathetic (vagal) effects. These effects are based on conditions of the human autonomic activities, such as assuming an upright position, mental stress and exercise, which are associated with an augmentation of sympathetic tone. In contrast, parasympathetic tone is high during resting conditions and sleep. So the activation of the sympathetic part leads to tachycardia and the activation of the parasympathetic part leads to bradycardia. Hence, the neural regulation of circulatory function is mainly effected through the interplay of the sympathetic and parasympathetic outflows. These two parts are in a reciprocal relation, which means the activation of either one results in the inhibition of the other one. [9, 10, 11, 12]

The effects of the sympathetic and parasympathetic part onto the cardiovascular system can also be described, based on the intrinsic heart rate. This is the heart rate (HR) measured in absence of sympathetic and parasympathetic influence, due to denervation or pharmacologic blockade [7, 13].The intrinsic HR is approximately 100-120 beats/min in a healthy human subject. Now it is possible to slow down or accelerate the HR by exciting the corresponding part. The sympathetic activation is triggered via circulating epinephrine, neural release of norepinephrine, or both and the parasympathetic activation via acetylcholine release from efferent vagal nerve discharge [14].

An increment of the HR could occur, because of a sympathetic effect, or a decremented parasympathetic effect e.g. because of a vagus-block. Normally the main part for incrementing the HR above the intrinsic HR is the sympathetic one, with a 5 seconds delay until the increment-effect occurs. After the next 20-30 seconds the heart gets into a "steady state", which means the effect of further sympathetic impulses is inhibited. In contrast, the sinus node answers with much less delay, if parasympathetic impulses appear. With this concept it is possible to measure the sympathetic and parasympathetic effects independently [8].

2 Methods

At the beginning, a literature study of different direct and indirect methods on the usability and the implementation possibilities in this work was realized. There are several physiological signals and parameters for monitoring the driver's alertness level, like the brain activity (EEG)[15] , the rate of eye closure (PERCLOS) [16], the ECG[17], vision based detection for detecting blinking and yawning[18] and the skin conductance/resistance[19]. For analyzing human alertness through the changes of the vehicle parameters, important signals are the steering wheel movements [20], the lane tracking and the pedal operation [21]. As mentioned in the introduction, the HRV was chosen for the direct measure of the driver´s drowsiness level. As published in [22] and [17] a correlation between subjective drowsiness evaluation and certain heart rate variability measures was found. The fact that [23] published indices in the HRV, which correlate with the alpha power of the EEG energy during the transition from awake to sleep, confirms the use of the HRV in this work. As no study was found, in which the ECG of subjects was monitored during long sleep deprivation, the study "Reaction time determination during sleep deprivation" was implemented.

For analyzing the methods of the indirect approach, the steering wheel movements, different algorithms and calculations were implemented. So the analysis of the power spectrum density (PSD), the spectrogram, the Steering Wheel Reversal Rate (SRR) and the Steering Interval Time (SIT) could be executed.

Data analysis and visualization was done with MATLAB® (Mathworks Inc., Natick, USA).

2.1 Implementation of the driving study

A commercial vehicle from the manufacturer MAN®was used to carry out the measurements. Detailed information about the test vehicle is listed in table 2.

Manufacturer	MAN AG
Type	TGA 18.430
Axle designation	4x2 (4 wheels, 2 powered)
Hirer	Eibinger Transportion
Registration date	2005
Odometer reading	787 500 km
Engine power	321 kW
Overall weight	7.5t (18t gross load weight)
Transmission	16 gear, manual

Table 2: Information test vehicle

Figure 2: MAN TGA 18.430

To ensure a realistic surrounding, which is comparable to the working environment of a professional truck driver, the trailer was loaded to the maximum allowed overall weight of 40 tons by loading steel beams, which, at the same time had the advantage of giving the trailer a deep balance point. The trip included motorways and national highways with an appropriate mixture of straights and curves, inclines and declines.

Figure 3: The inside of the trailer with the loaded steel beams

For measuring the steering activity of the test driver a wire rope potentiometer (”Posiwire®WS10SG from ASM®) was connected to the steering rod.

Figure 4: Wire rope potentiometer

The aim of the test rides was to record driver´s reaction during a normal working day of a professional truck driver. Therefore several test rides were performed on two different selected routes which were located in Austria and Germany. The first route had a length of 554 km

and was accomplished within 7 hours. The second route with a length of 340 km needed a drive-time of about 4 hours and 30 minutes.

Two different circular courses, one in Austria and the other one in Germany were used to perform the test rides. The detailed routes are displayed in figure 5 and 6, with additional information of the street names.

Route in Austria

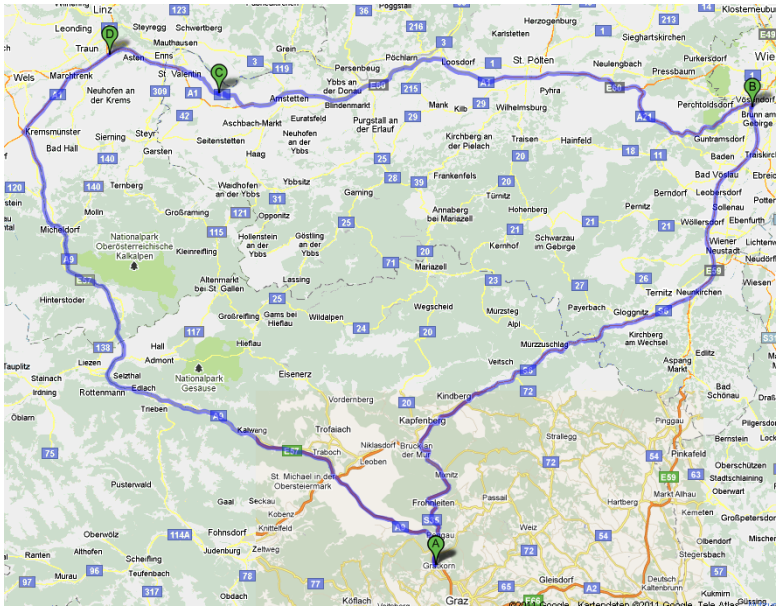

Figure 5: Driven route in Austria

Detailed information of this route are described in the following table.

Part of the route	Street name	Marker
Graz/Gratkorn - Wien	A9 - S35 - S6 - A2	A - B
Wien - Strengberg	A21 - A1	B - C
Strengberg - Linz	A1	C - D
Linz - Sattledt - Gratkorn	S6	D - A

Table 3: Characteristics of the route in Austria

Route in Germany

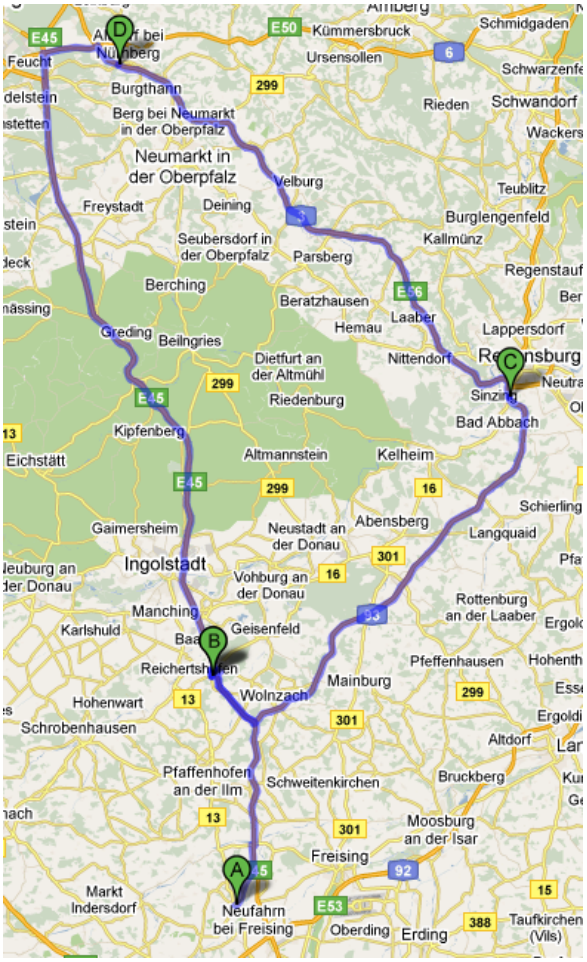

Figure 6: Driven route in Germany

Part of the route	Street name	Marker
Fahrenzhausen - Pfaffenhofen - Langenbruck	B13 - B300	A - B
Langenbruck - Autobahnkreuz Hallertau - Regensburg	A9 - A93	B - C
Regensburg - Altdorf bei Nürnberg	A3	C - D
Altdorf - Langenbruck	A3 - A6 - A9	D - B
Langenbruck - Fahrenzhausen	B300 - B13	B - A

Table 4: Characteristics of the route in Germany

2.2 Implementation of the reaction time study

For analyzing the reaction time (RT) during sleep deprivation 12 male test subjects participated in this study (age range 25.5 ± 1.5 years (mean $\pm$ SD)).

The ECG from each subject was recorded during 20 hours, from 10 am to 6 pm the next day. Each recording period was divided into 2 phases. The first phase (10am to 22pm) had a length of 12 hours and the second one 8 hours (22pm to 6am). In the first phase the test subjects were asked to pass a "normal day" without ingestion of stimulating substances (e.g. caffein) and without extreme physiological exercise. In the second phase the subjects had to make a reaction test and give a subjective drowsiness rating every 30 minutes. Written informed consent was obtained from all subjects. Furthermore they were informed about the possibilty to abort the study process at any time without any reason. This agreement is attached as Appendix A (written in german).

2.3 Measurement of the ECG

In both of the studies an ECG Monitor was attached to the subject to obtain the HRV. More precisely, the ECG Monitor measures the heart cycles, from which the RR-Intervals were extracted for the HRV Analysis.

The used ECG montitor was a "Schiller Medilog AR12®". The specifications are listed in table 5 and the device is presented in figure 7.

Size(HxWxL)	70x100x22
Number of Electrodes	5
ECG channels	3
Sampling frequency	4096 Hz
Resolution	16 bit

Table 5: Specification of ECG monitor "Schiller Medilog AR12®"

The applied ECG monitor uses the lead-configuration according to Nehb , which is a modification of the Einthoven leads. The Nehb-configuration lead is a bipolar system which is also called "small heart triangle". It can be seen as a an adjustment of the Einthoven triangle, where the electrodes are moved from the extremities to the chest[5].

Figure 7: Schiller Medilog AR12®

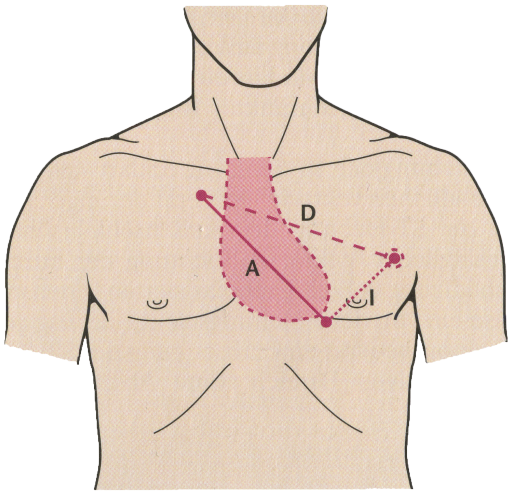

Figure 8: Projections of the Nehb-configuration lead

Figure 8, taken from [5], depicts the lead-configuration of the Nehb system. The A (anterior) lead reflects the electrical actions of the anterior wall and the I (interior) lead the electrical

actions of the heart-sections near the diaphragm. The D (dorsal) lead registers additional impulses from the posterior wall.

2.4 Measurement of the HRV

Generally, the heart rate variability can be evaluated through a time-domain or through a frequency-domain method. Both of these two methods can be further divided in more specific indices, in order to get the best results for the individual measurement situation.

2.4.1 Time domain

When analyzing the HRV in the time-domain method, either the beat to beat interval at any point in time directly, or the variance between successive beat to beat intervals are determined. In a continuous ECG record, each QRS Complex is registered and with this information, the beat to beat interval or the time variance of successive beat to beat intervals can be determined. The beat to beat interval is also known as normal-to-normal interval (NN-Interval) and describes the time between subsequent depolarization waves, due to the sinus node activation. In contrast to the Task Force, the NN-Interval will be noted as RR-Interval, from now. The time- variance of successive beat to beat intervals is also known as the differences between adjacent RR-Intervals. Measures that are based on the RR-Interval directly do not distinguish the autonomic sources, such as rest, sleep, tilt, valsalva maneuver and have therefore no significance for this study [24].

From a series of many RR-Intervals, recorded over a longer period of time, there is the possibility of further analyzing methods in the time domain, which can be named "statistical methods". It is possible to analyze long term recordings in both mentioned ways, but for the aim of this study the method of analyzing differences between adjacent RR-Intervals seems more promising, due to the relationship with the autonomic nervous system. Another disadvantageous aspect of the direct RR-Interval analysis is the fact, that this analysis method has a relation with the length

of the ECG recording[4]. One simple approach is to calculate the standard deviation of the RR-Intervals (SD_{RR}), which is the square root of the variance (Equation 4). Since the variance is mathematically equal to the total power of the spectrum, SD_{RR} reflects all cyclic components, which are responsible for the variability in the period of the recording. So, only with recordings of the same length, typically 24 hours, it is possible to compare them properly. For this reason the SD_{RR}, should be calculated over short periods, like 5 minutes, in a long term recording.

$$SD_{RR} = \sqrt{\frac{1}{N-1}\sum_{i=1}^{N}(RR_i - \overline{RR})^2} \tag{4}$$

where N is the number of registered beats in the recording, and

$$\overline{RR} = \frac{1}{N}\sum_{i=1}^{N} RR_i \tag{5}$$

The second type of indices, which are more adjuvant for this study, are the indices using the differences between adjacent RR-Intervals. Two valuable indices of this type are the root mean square of differences between adjacent RR-Intervals - RMSSD (4) and the percentage of pairs of adjacent RR-Intervals differing more than 50ms - pNN50 (5).

$$RMSSD = \sqrt{\frac{1}{N}\sum_{i=1}^{N}(RR_{i+1} - RR_i)^2} \tag{6}$$

where $(RR_{i+1} - RR_i)$ describes the difference between adjacent RR- Intervals

$$pNN50 = \frac{N_{RR,50}}{N_{ges}} \cdot 100 \tag{7}$$

$N_{RR,50}$ stands for the number of pairs of adjacent RR-Intervals differing by more than 50ms

These indices are calculated in certain time windows. The length of one window varies between

2 and 5 minutes, in order to get the best balance between the overall length of the recording and the time window. The proper choice of the window length is crucial for the accurate estimation of both the short- and longterm oscillations in the HRV. It should be noted that the RMSSD is the most commonly used value for analyzing interval differences. This method acts like a high-pass filter, hence it removes long term trends and lower frequency variability from the data.

Another analyzing approach, according to the time domain, are the geometrical methods. The point of origin of these geometrical measures is the histogram of all RR-Intervals in one recording. The recordings, which are analyzed by geometrical measures should have an appropriate number of RR-Intervals to ensure the correct performance of this method.

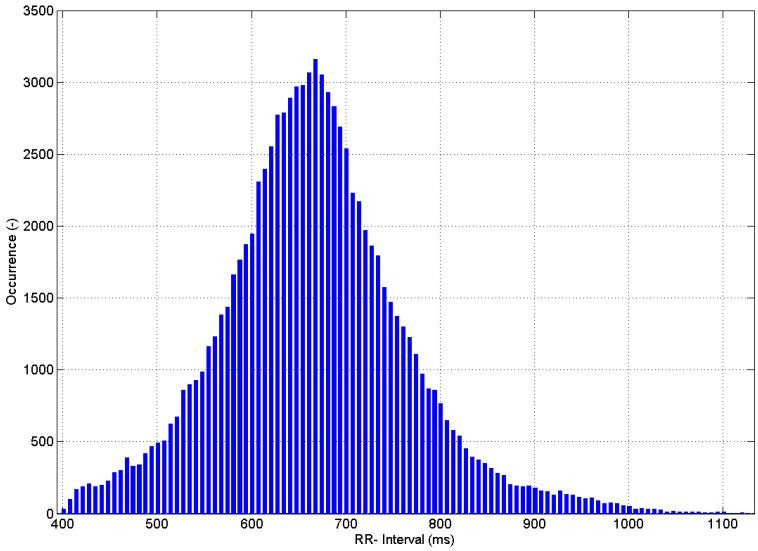

Figure 9: RR-Interval histogram

Figure 9, displays the time length of the RR-Intervals on the horizontal axis and the corresponding number of occurences of the RR-Intervals on the vertical axis.

As mentioned before, these geometry based indices are calculated over a whole recorded data set, and have no information of short-term changes in the HRV. The interest in short term changes in HRV in this study, excludes the use of geometry based indices. For a detailed explanation about the geometrical methods please refer to [4].

2.4.2 Frequency domain

In relation to the chapter 'Structure' the sympathetic and parasympathetic influence on the frequency spectrum of the HRV is of interest. As briefly mentioned in the introduction to the HRV, the respiratory sinus arrhythmia (RSA) that contains both, the respiratory frequency and the variability related to blood pressure fluctuation, characterized by a frequency of about 0.25 Hz, is one important frequency component. The second important frequency component, is related to the blood pressure and is known as Mayer-wave related sinus arrhythmia (MWSA), with a frequency component of about 0.1 Hz [3]. Furthermore two more components related to much lower frequencies (< 0.3 Hz) can be recognized. The one is a band between 0.003 and 0.04 Hz, which is related to thermoregulatory systems and known as very low frequency band(VLF). The VLF component is often subtracted from the total power, because it appears relatively unstable and rarely is of diagnostic relevance in analyzing HRV. The other is an even slower component, which appears below 0.003 Hz and is known as ultra low frequency band (ULF). This ULF was shown to be useful for predicting the tendency of morbidity and mortality, which appears to arise from a relation with the functional capacity[3] of the patient[24].

The MWSA and the RSA related frequency bands have been commonly labeled as low-frequency (LF) and high-frequency (HF) component of the HRV. There is a relatively high acceptance that the HF component can be regarded as a reliable marker of vagal activity[12]. However, there is a little controversy about the LF component. Some authors consider the LF component as marker for symphatetic activity while others consider the LF component as index for both sympathetic and parasympathetic activities[3].

In this context the LF to HF ratio can be explained in two ways. The LF/HF ratio can be a marker of sympathetic and parasympathetic activities. This is the case, if the LF is considered just as an index of sympathetic responses. The LF/HF ratio can also be understood as a marker of sympathetic activities. LF is then considered as an index of both sympathetic and parasympathetic responses, because the dividing factor HF will eliminate or at least minimize the effect of the parasympathetic response.

[3]Functional capacity refers to the capability of performing tasks and activities that people find necessary or desirable in their lives

Through the Power spectral density (PSD) it is possible to describe, how the power density of a time series is distributed with the frequency. There are generally two concepts of calculating the PSD, the nonparametric and the parametric methods. Nonparametric methods estimate the PSD directly from the signal itself. The simplest such method is the periodogram. An improved version of the periodogram is Welch's method.

Welch's method for estimating power spectra is carried out by dividing the time signal into successive blocks, forming the periodogram for each block, and averaging.

The m-th windowed, zero-padded frame of the signal x is denoted by

$$x_m(n) \mathrel{\widehat{=}} w(n)x(n + mR); \tag{8}$$

$$\text{with n=0,1,...,M-1 and m=0,1,...,K-1}$$

Where R is defined as the window hop size (number of samples between successive FFT windows) and K denotes the number of of available frames. Then the periodogram of the m-th block is given by

$$Px_m \mathrel{\widehat{=}} \frac{1}{M}|\sum_{n=0}^{N-1} x_m(n)e^{-j2\pi nk/N}|^2 \tag{9}$$

where N denotes the length of the fourier transform.

Parametric methods are those in which the PSD is estimated from a signal that is assumed to be output of a linear system driven by white noise. Examples are the Yule-Walker autoregressive (AR) method and the Burg method. These methods estimate the PSD by first estimating the parameters (coefficients) of the linear system that hypothetically generates the signal. They tend to produce better results than classical nonparametric methods when the data length of the available signal is relatively short[25]. The main advantage of the used Burg method is that it has a high resolution for short data records, and it always produces a stable model.

All parametric methods yield a PSD estimate given by

$$Px(w) \widehat{=} \frac{1}{f_s} \frac{\epsilon_p}{|1 + \sum_{k=1}^{p} \widehat{a}_p(k) e^{jwk/f_s}|^2} \tag{10}$$

Where the $\widehat{a}_p(k)$ are the estimates of the parametric parameters obtained from the Levinson-Durbin recursion. ϵ_p are reflection coefficients in an equivalent lattice structure, which are chosen to obtain the total least squares error.

Once the RR-Interval time series has been transformed to the frequency domain, by either Welch´s or Burg´s method, there are mainly three frequency ranges, which reflect a relationship with the ANS. These three frequency components are calculated by short term windows like 2 to 5 minutes of the recording. The tree components are the very low frequency (VLF), the low frequency (LF) and the high frequency (HF) bands. These VLF, LF and HF components can be presented in absolute units (ms^2) and the LF and HF can also be presented in normalized units (nu). As the Equation 11 shows, the normalized units subtract the VLF-power from the particular frequency range. By converting the frequency components to normalized units, the reciprocal relation between the two counterparts of the ANS is more clearly. Also changes in the whole spectrum minimize the effect on the LF and HF components, if the units are normalized [4, 8].

$$P(nu) = \frac{P(ms^2)}{\sigma^2(ms^2) - P_{VLF}(ms^2)} \cdot 100 \tag{11}$$

P is the power of the LF or HF part, σ^2 is the total power and P_{VLF} indicates the power of the VLF component.

2.5 Steering signal

Steering denotes the lateral navigation of the vehicle, assuming the speed is not zero. As mentioned in chapter 2 the indirect approach for measuring the driver fatigue are the steering wheel movements. The operation of the steering wheel can be seen as elementary interface between the driver and the vehicle. Special characteristics of the steering wheel movements

reflect various conditions of the driver. Hence the signal of the steering wheel movements is a useful value for describing the drowsiness level of the driver. The steering signal includes suitable information in time and frequency domain, which are analysed by selected methods.

2.6 Steering signal - frequency domain

A tool for analyzing non-stationary signals is the short time fourier transform (STFT). A stationary signal is defined as a stochastic process whose probability density function does not change when shifted in time or space. Consequently a non-stationary signal is defined as signal, which does not obey to these requirement.

2.6.1 Short time fourier transform

The normal fourier transforms give no clear information on the change of the frequeny component over the time. To get this information the signal is divided into blocks, in which the spectrum is calculated separately.

$$X[n,\lambda) = STFT(x[m]) \mathrel{\widehat{=}} DTFT(x[m+n]w[m]) \tag{12}$$

$$X[n,\lambda) = \sum_{m=-\infty}^{\infty} x[m+n]w[m]e^{-j\lambda m} \tag{13}$$

$$with\ m,n \in \mathbb{Z}\ and\ \lambda \in \mathbb{R}$$

where the block length is determined by the window function $w[m]$ of length L

$$X(n,\lambda) = \sum_{m=0}^{L-1} x[m+n]w[m]e^{-j\lambda m} \tag{14}$$

The discrete STFT is calculated by: $\lambda \rightarrow k$ with $\lambda_k = \frac{2\pi}{N}k$ and from that,

$$X[n, \frac{2\pi}{N}k] = \sum_{m=0}^{L-1} x[m+n]w[m]e^{-\frac{2\pi}{N}km} \tag{15}$$
$$with\ 0 \leq k < N$$

results, which means that the frequency axis is divided into N equally spaced samples from 0 to 2π.

The STFT can be visualized by a so called spectrogram, which is expressed by

$$spectrogram\{X[n]\} \equiv |X[n, \lambda]|^2 \tag{16}$$

With this method it is possible to detect discontinuities in the frequency domain at the corresponding number of samples, which can be traced back to the according point of time.

2.6.2 Spectral analysis

As described in [21] the power ratio of related frequency bands of the steering angle signal, can be used to charaterize the driver´s steering operations.

The spectrum is divided into three bands:

- road shape component (0 - 0.1 Hz)
- predictive component (0.1 - 0.3 Hz)
- corrective component (0.3 - 1 Hz)

The thresholds were received in a precious study with test drives, were the drivers were restricted in their field of view. By changing the lower and upper boundary of the restricted view, the

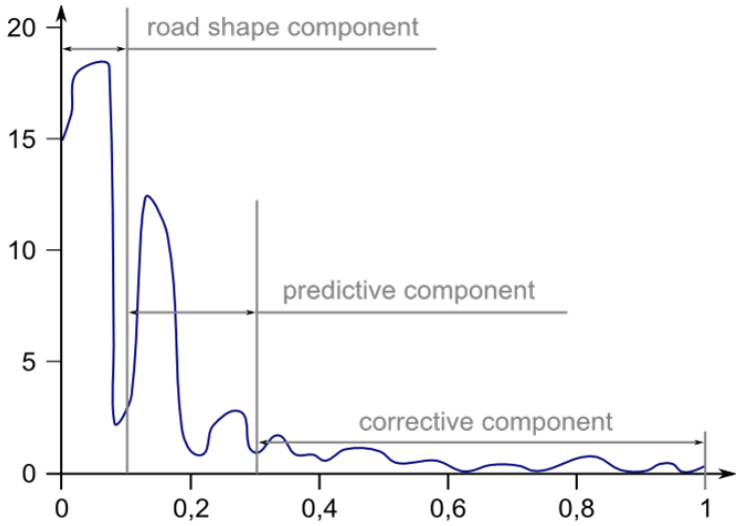

Figure 10: Frequency components of the steering angle signal

changes in steering operations were analyzed. Hence, the listed frequency bands were obtained [21].

These frequency bands are useful to eliminate the road shape component from the steering signal. This is helpful, because the steering actions, which are required to navigate through different curves to keep the vehicle on the road, can be minimized. With this achievement the steering signal includes just components which are required to keep the vehicle between the road boundaries, independet of the course of the road.

The remaining frequency bands (predictive and corrective) can also be used to characterize the steering behavior of the driver. This was realized by comparing the frequency bands of one driver of the same course, but on different dates.

2.7 Steering signal - time domain

2.7.1 Steering wheel reversal rate

As stated by [26] the steering behaviour of an alert and a drowsy driver differs in time. More precisely an alert driver handles the steering wheel skillfully with continuous changes of steer-

ing wheel angles, which reflects control operations to keep the vehicle within the specified road boundary. In contrast, a drowsy driver holds the steering wheel with less and inelastic movements for a longer period fowolled by sharp turns, keeping the vehicle on the intended road. This observation can be quantified with the so called Steering wheel reversal rate (SRR). The SRR specifies the number of times, in a certain time interval, in which the steering angle is reversed within a certain threshold. Thus, a high SRR should indicate an alert and fit driver, in comparison to a low SRR which should indicate a drowsy and/or distracted driver. This threshold of the steering angle is defined by the parameter gap size, which can be specified individually. In [21] the best results were achieved with a gap size of 10 degrees.

In figure 11, 3 reversals $\Delta\delta_1, \Delta\delta_2$ and $\Delta\delta_3$ are displayed, which are exceeding the threshold (in this case 8 degrees) in a time interval of approximately 6 seconds. During driving over a longer period of time, like e.g. 8 hours, the amount of reversals can be tracked during many intervals with the same duration. The intended purpose of this index is, to assess the decrease of control capability of the driver during increasing drowsiness.

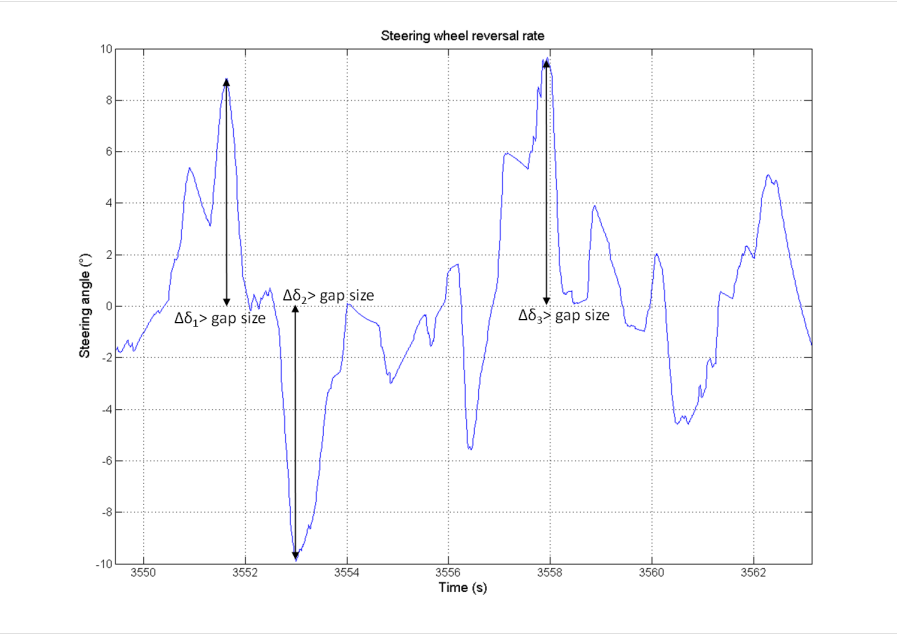

Figure 11: Steering wheel reversal rate

As already mentioned, the rate of the steering reversals is computed in time-windows, the length of which can be chosen. Also the applied gap size, at which a steering reversal is counted, can be regulated. By analyzing the steering angle signals, with different settings of gap size and window length, differences can be detected.

2.7.2 Steering interval time

As proposed by [27] the interval between consecutive steering adjustments is prolonged, if the drowsiness level of the driver is increased. The gap size, as introduced in the previous chapter (SRR), is now used to to analyze the time interval between steering adjustments. This was implemented by measuring the time intervals, in which the steering angle is not exceeding the predefined gap size. This time interval is called the "subthreshold interval".

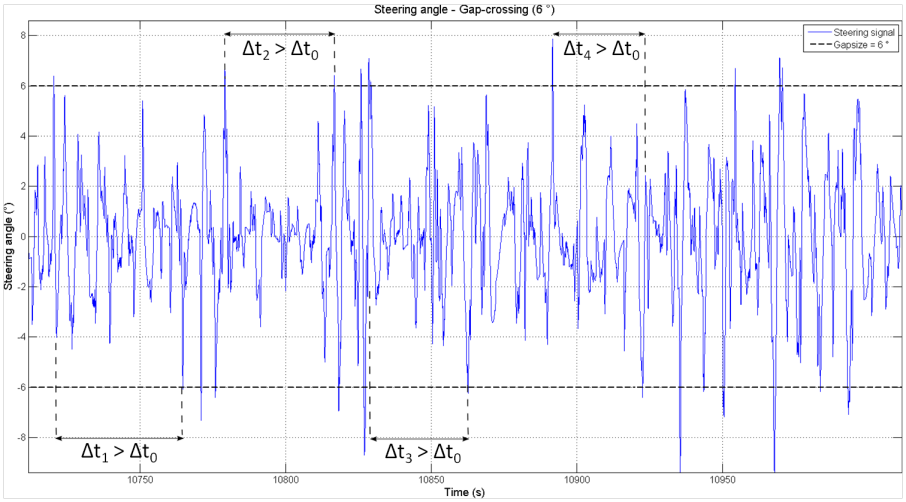

Figure 12: Steering interval time

In figure 12, Δt_0 is the minimum non overstepping time and Δt_1 to Δt_4 are the steering intervals, in which the minimum subthreshold interval is overstepped.

For further analysis, the subthreshold interval and the corresponding gap size can be adjusted. Analogue to the computation of the SRR, the settings for the steering interval time can be modified, in order to see which parameters give the most promising results.

2.8 Reaction time determination

Taken from [28], the reaction time (RT) is made up of the decision and the motoric time. The decision time is the time interval between the occurrence of an event and the start of the first ensuing action. The motoric time is the interval between starting and finishing the first ensuing action.

The event in this case is an optical and/or acoustical stimulus. To measure the decision time with the RT test program, a normal computer keyboard is used. Therefore the test subject presses the space bar and has to release the finger after recognizing an event to press the enter button. The time from recognizing the optical/acoustical event to releasing the space bar is the decision time. The time intervall between releasing the space bar and pressing the enter button is the motoric time.

Although it is not possible to transform these actions on the keyboard to corresponding situations in the traffic, an rude interpretation can be made. Hence the decision time, which is the time from the event to the release of the space bar, would correspond to the time from recognizing a dangerous situation to starting the movement of the foot towards the break pedal. The interval from starting the movement of the foot till pressing the break pedal, can be interpreted as interval from releasing the space bar till pressing the enter button in the RT test program. A braking maneuver in a vehicle consists of more time intervals, after the decision and motoric time, there is the operating time and the dwell time. The operating time is the period from pressing the break pedal to the first braking effect of the vehicle and the dwell time is the period from the beginning of the braking effect to the complete braking effect[28]. As the last two periods are mainly influenced by the performance of the vehicle´s breaking system itself, fast reaction time of the driver is crucial in a dangerous situation.

2.8.1 Reaction time- test program

The events, to which the subjects had to respond, were a combination of optical and acoustical stimuli. To keep the training effect at a low level, the events were varied through the different

options.

In one variant of the test, the subjects hat to react to the appearance of a yellow circle and a simultaneous acoustic singnal (Figure 13).

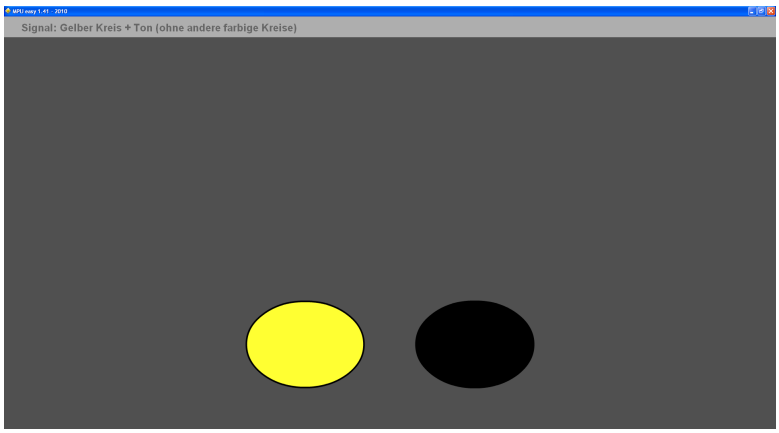

Figure 13: First variant of the reaction test

The second variant was the occurence of one yellow and one red circle simultaneously (Figure 14).

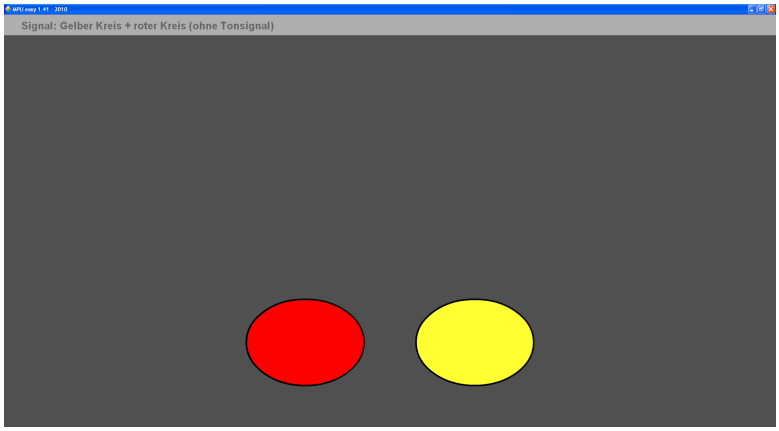

Figure 14: Second variant of the reaction test

The third variant was the fusion of variant one and two, which means the subject had to respond to both of the explained stimuli.

Every 30 minutes this test was done for 6 minutes by the subject. From that, the decision time, the motoric time and the sum of them, the reaction time, was determined.

2.8.2 Stanford sleepiness scale

As briefly explained in the introduction, the Stanford sleepiness scale (SSS) is a tool to document the subjective level of drowsiness. The scale has 8 digits, starting from 1 (wide awake) to 7 (sleep onset soon), the last digit is "asleep" and is written as "X". The complete Stanford sleepiness scale is illustrated in table 6.

Degree of Sleepiness	Scale Rating
Feeling active, vital, alert, or wide awake	1
Functioning at high levels, but not a peak; able to concentrate	2
Awake, but relaxed; responsive but not fully alert	3
Somewhat foggy, let down	4
Foggy, losing interest in remaining awake; slowed down	5
Sleepy, woozy, fighting sleep; prefer to lie down	6
No longer fighting sleep, sleep onset soon; having dream-like thoughts	7
Asleep	X

Table 6: Stanford sleepiness scale

The progression of the subjective drowsiness rating, will be taken as a supporting indication for the direct and indirect measurement of drowsiness. To fulfill this assignment the test subjects made a rating according to the SSS every 30 minutes, in the driving study and in the reaction time study.

2.8.3 Cross correlation

To detect relationships between the above described indices, the cross correlation was used. The cross correlation is a measure of the similarity between two different signals. Equation 17

shows the cross correlation for continuous functions and equation 18 for discrete functions.

$$Corr(f(t), g(t)) \mathrel{\widehat{=}} \int_{-\infty}^{\infty} f^*(\tau) \cdot g(t+\tau) d\tau \tag{17}$$

$$Corr(f[n], g[n]) \mathrel{\widehat{=}} \sum_{m=-\infty}^{\infty} f^*[n] \cdot g[n+m] \tag{18}$$

where f^* denotes the complex conjugate of f.

The correlation coefficient r is defined as:

$$r_{corr(fg)} = \frac{\sum_{i=0}^{n}(f_i - \overline{f})(g_i - \overline{g})}{\sqrt{\sum_{i=0}^{n}(f_i - \overline{f})^2 \sum_{i=0}^{n}(g_i - \overline{g})^2}} \tag{19}$$

which

2.8.4 Cluster analysis

The purpose of cluster analysis is to organize an amount of data into groups with high similarity within each group and with low similarity to other groups.

In order to give a statement, if the measured and logged data represent the drowsiness level of the subjects sufficiently, a cluster analysis was executed. The intention of this clustering was to classify the 12 subjects into a group of considerable responders and into a group of non-considerable responders.

K-means algorithmus

The cluster analysis was realized with the "K- means algorithmus", the operating steps of which are:

1. The number of clusters 'k' has to be specified
2. The k-cluster centroids are randomly chosen
3. Each element is attributed to the cluster with the nearest centroid. Therefore a distance function is needed, which was realized with the 'Euclidean difference'(Equation 20).

$$d_{rs}^2 = (x_r - x_s)' \cdot (x_r - x_s) \tag{20}$$

4. The centroid for each cluster is newly calculated, so that it lies in the center of the cluster
5. Based on the newly calulated centroids, the elements are attributed to the clusters as in step 3, until the elements are not attributed to a new cluster anymore and the centroids stay the same

The data set, which is analyzed by the "k means algorithmus", includes the correlation coefficient between all pairs of parameters in the reaction time study. As there are 3 logged values (HRV, RT, SSS), the graph of the cluster analysis has 3 dimensions. This is illustrated with a three-dimensional scatter plot.

Dendrogram interpretation

As another graphical illustration of the cluster analysis the dendrogram can be used. Based on the 'Euclidean difference' between the different elements (the correlations of the 12 subjects in this case), a hierarchical system is formed, through the successive grouping of near elements, in order to combine them in bigger groups. The aggregation starts with combining the two elements with the shortest distance to a group. After that pairs of groups and/or elements with the shortest distance to each other are combined to a new group. After every grouping process a new distance is calculated, according to the aggregation of elements and/or groups in the step before. In every aggregation step a new group is generated, which is always bigger then the one

before. This process goes on till the n- elements are combined in one group, which occurs after n-1 steps. There are several options how the distance between the elements is used to form the groups. The 'single linkage' method uses the minimum distance: The distance between two groups is equal to the minimum distance of two elements from each group. The 'complete linkage' method works the other way around: The distance between two groups is equal to the maximum distance of two elements from each group. A compromise of these methods is the 'average linkage' method: The distance between two groups is the mean of the differences between all pairs of elements. For this work, the dendrogram was calculated by using the 'complete linkage' method, in order to generate clusters with the smallest possible variation.

3 Results

3.1 Driving study

The results of the driving study will be illustrated with selected examples. The reason of that is the small number of test subjects involved. Therefore the subjective rating of sleepiness (SSS) is taken as an indicating value, at which period or instant of time, the driver had an increased fatigue level. On this base, the recorded data of the heart rate variability and the steering signal were analyzed by the stated methods. The two drivers will be noted as "Subject 1" and "Subject 2" in the further sections.

3.1.1 Stanford Sleepines Scale

There were two notable test rides, in which an increased level of fatigue was specified with the SSS. Ratings with a scale of at least "4" were considered, which is described as "Somewhat foggy, let down" by the SSS.

This two cases of increased fatigue, will be labeled as 'case 1' and 'case 2' in the further sections. The details of these two cases are listed in Table 7 and 8. The progression of the SSS is displayed in figure 15 for case 1 and in figure 16 for case 2.

Case 1

Driver	Subject 1
Route	Graz (Styria) - Strengberg (Lower Austria)
Date	July, 14. 2010
Time	10:15 - 14:00

Table 7: First appearance of an increased fatigue: case 1

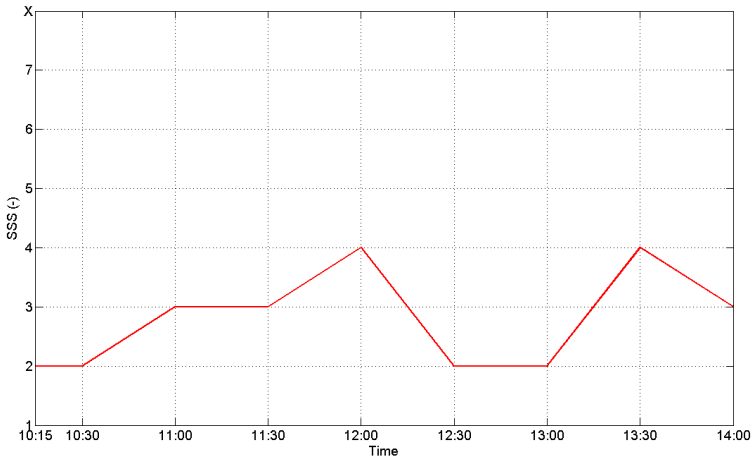

Figure 15: Stanford Sleepines Scale of case 1

Case 2

Driver	Subject 2
Route	Graz (Styria) - Guntramsdorf (Lower Austria)
Date	July, 20. 2010
Time	9:00 - 11:00

Table 8: Second appearance of an increased fatigue: case 2

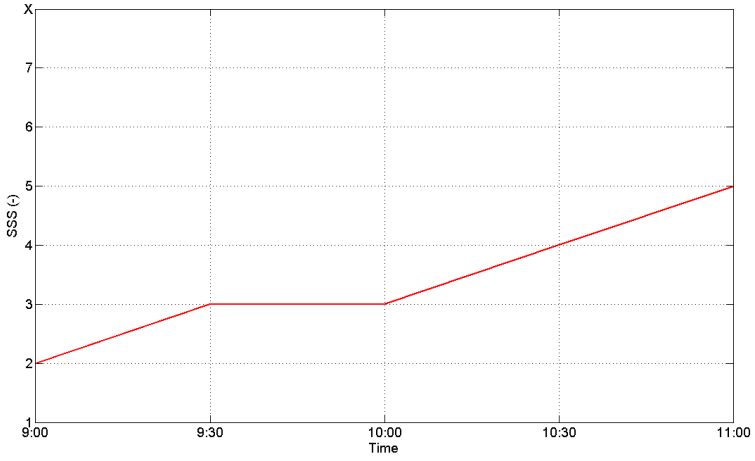

Figure 16: Stanford Sleepines Scale of case 2

3.1.2 HRV values

Case 1: HRV time domain indices

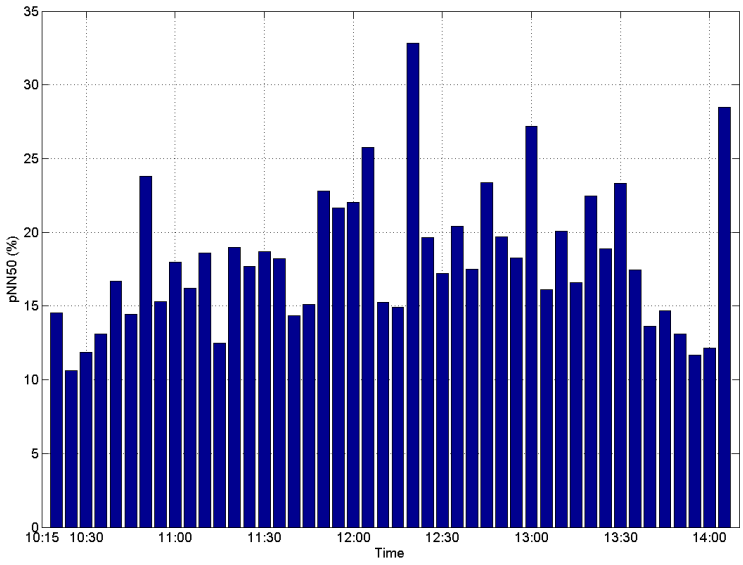

Figure 17: pNN50 Value of case 1

Here, no particular variation of the pNN50 is observable. At 12:00 and at 13:30, the driver made a SSS-rating of 4, which can not be detected with the pNN50 value.

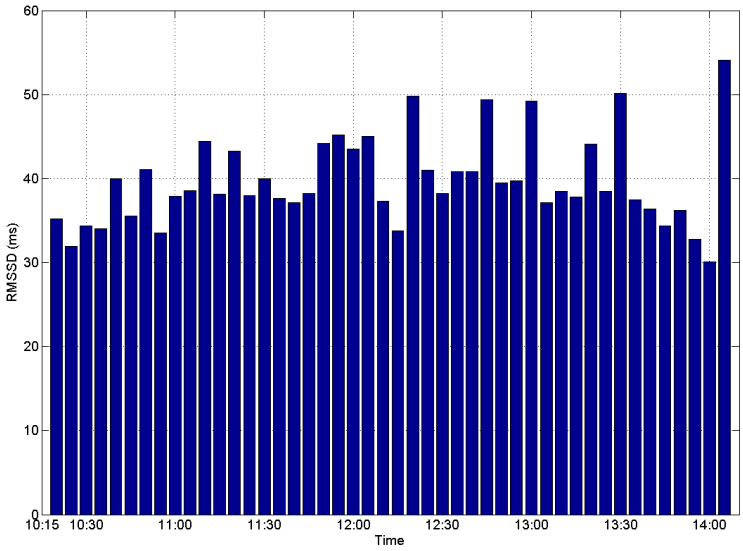

Figure 18: RMSSD Value of case 1

Also the RMSSD shows no particular variation and no relationship with the SSS-rating.

For analyzing the HRV in the frequency domain, the next figure shows the low-frequency to high-frequency ratio, which was used for analyzing the HRV in the frequency domain.

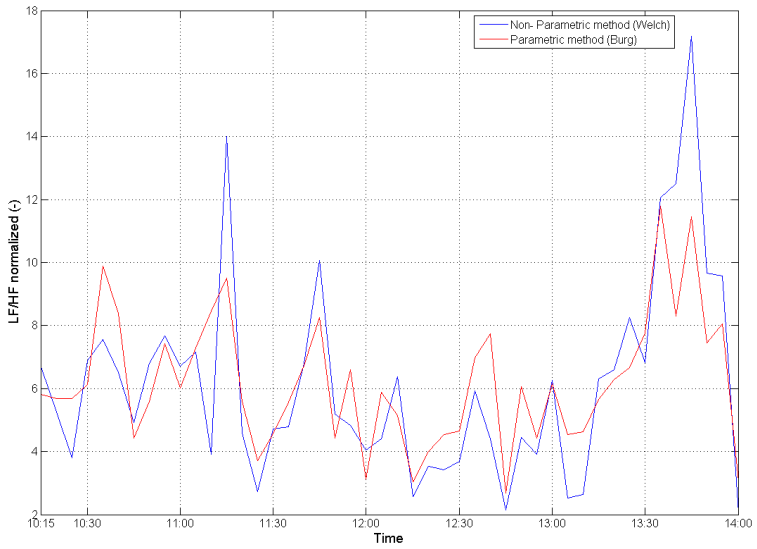

Figure 19: LF/HF ratio of case 1

Figure 19 displays the LF to HF ratio in normalized units. The values are calculated with both, the parametric (Burg) and the non-parametric method(Welch). A slight dissimilarity between the two transformation methods (Burg and Welch) is apparent, although the general trend is quite similar, the peaks of the welch method having a higher amplitude. For indicating the level of drowsiness, no method of the LF to HF ratio shows a trend according to the subjective drowsiness rating of the driver.

Case 2: HRV time domain indices

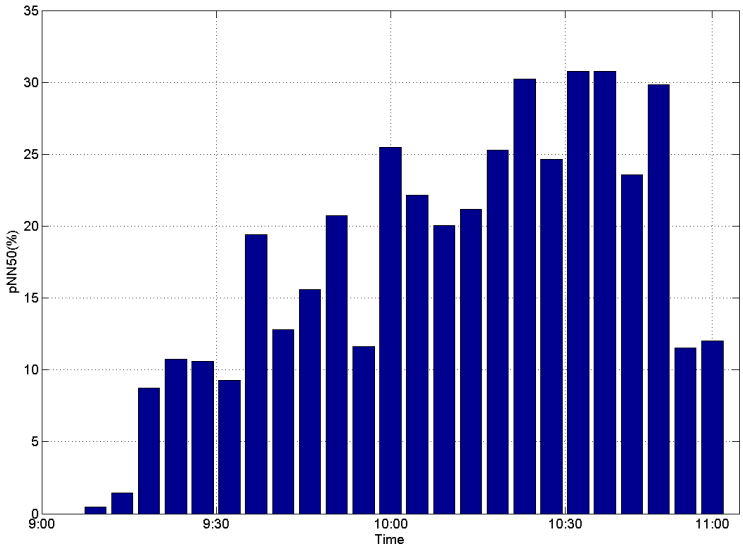

Figure 20: pNN50 Value of case 2

The pNN50 is continiously increasing during the test drive, as displayed in figure 20. The means of the pNN50, as seen in Table 9, also document this progression.

Time	Mean of pNN50 (%)
9:00 - 9:35	7.58
9:40 - 10:15	18.71
10:20 - 11:00	24.30

Table 9: Means of pNN50

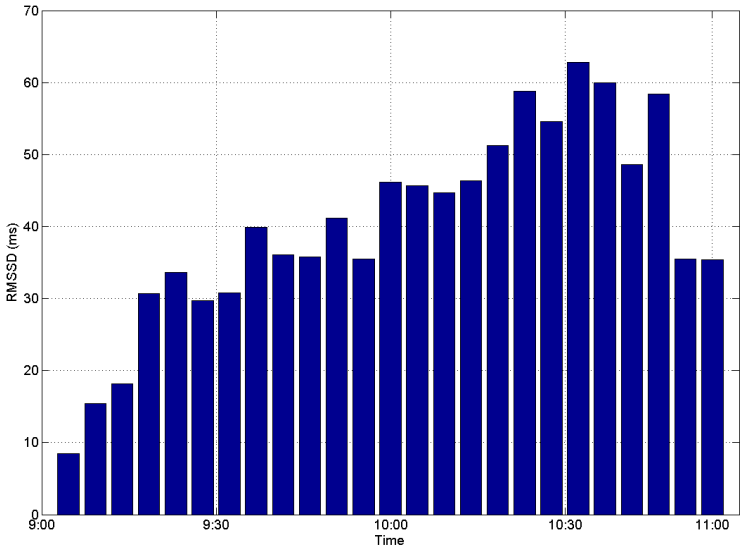

Figure 21: RMSSD Value of case 2

The RMSSD value is increasing during the drive, due the increasing fatigue indicated by the SSS. To ensure this fact means of the RMSSD are listed in Table 10.

Time	Mean of RMSSD (ms)
9:00 - 9:35	25.85
9:40 - 10:15	41.45
10:20 - 11:00	51.71

Table 10: Means of RMSSD

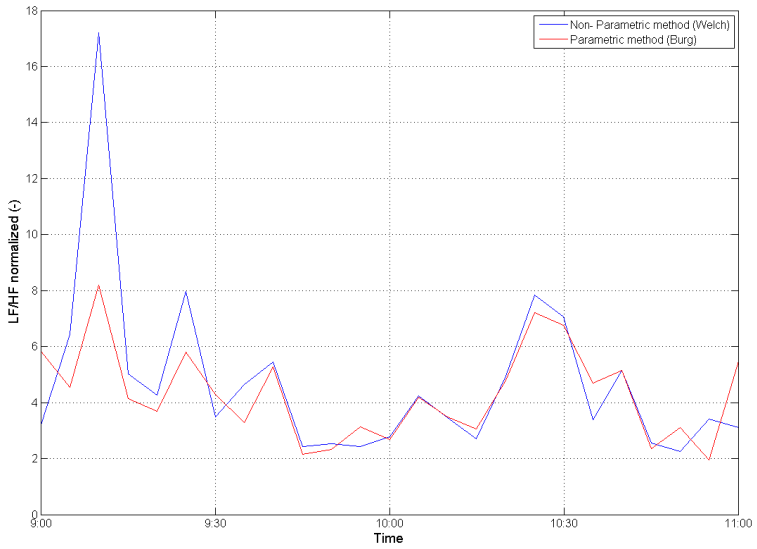

Figure 22: LF/HF ratio of case 2

As observable, the LF to Hf ratio gives not such a clear indication of increasing fatigue as seen with the time-domain indices. It was expected that the LF to HF ratio decreases continiuosly towards 11:00, due to an increasing HF and a decreasing LF. Nevertheless it is worth to mention that a decrease is evident from 10:25 to 11:00, when the amount of drowsiness was the highest according to the SSS. This effect is even more obvious using the parametric (Burg) method.

3.1.3 Steering Signal

Case 1: Steering Signal - Spectrogram

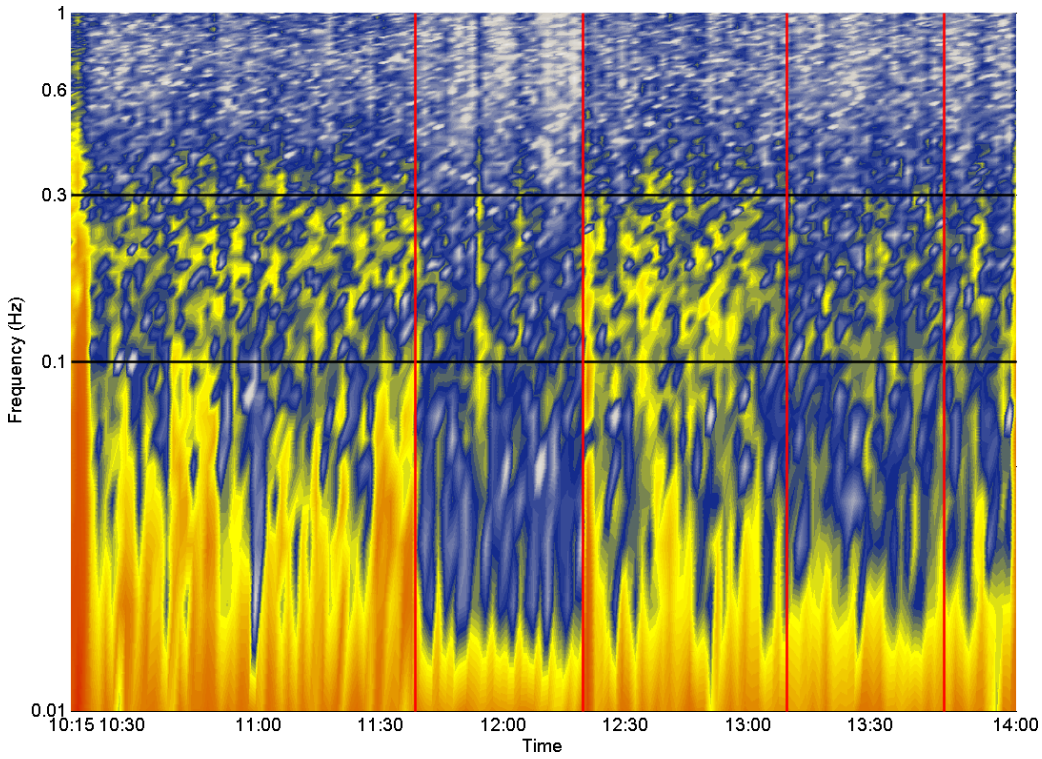

Figure 23: Frequency distribution of the steering behaviour of case 1

The horizontal axis describes the duration of the test ride and on the vertical axis the frequency of the steering wheel movements is plotted. The colour indicates the power of the frequency bands. Two periods of increased fatigue, in which Subject 1 made a SSS-rating of '4', are observable. This periods are indicated by the red vertical lines.

By analyzing the spectogram with the frequency components of the steering angle, as introduced in chapter 2.6.2, the following conclusions can be stated: The amount of steering behaviour in the corrective component (0.3 - 1 Hz) and also the predictive component (0.1 - 0.3 Hz) is decreased. Additionally a strong reduction of the steering frequency, down to approximately 0.02 Hz is evident, during the phases of increased fatigue.

Case 1: Steering Wheel Reversal Rate

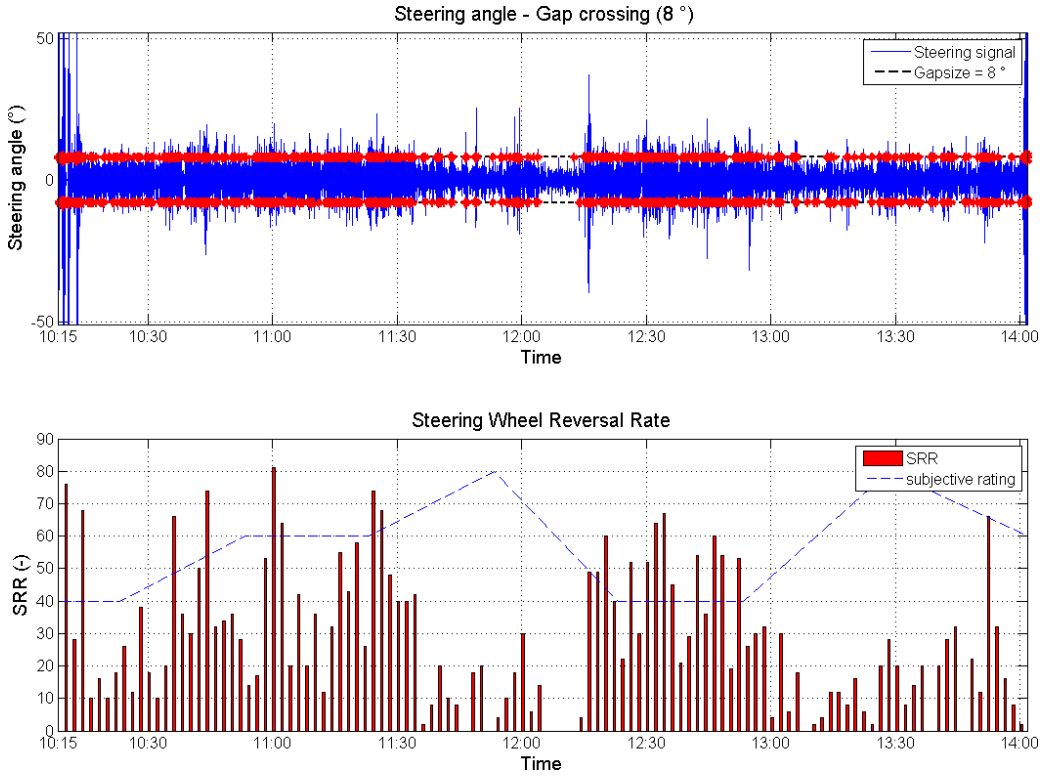

Figure 24: Steering wheel reversal rate

In the upper part of figure 24 the steering signal is plotted with the corresponding exceedings of the specified gapsize. The steering wheel reversal rate, as seen in the lower part of the figure, was calculated with a gapsize of 8 degrees in time windows of 2 minutes. With these settings the SRR shows the most promising results. Different values of the gap size (from 2 to 12 degrees) and the time window length (from 1 to 5 minutes) were tested, from which the used values were empirical chosen.

Analyzing the SRR, the occurrence of the two phases of fatigue can also be seen. A decreasing rate of the steering reversals coincides clearly with increasing fatigue. The SSS-rating is fitted into the plot for a easier comparison. Generally it is possible to observe, that the SSS-rating and the SRR have a reciprocal relation.

Case 1: Steering Interval Time

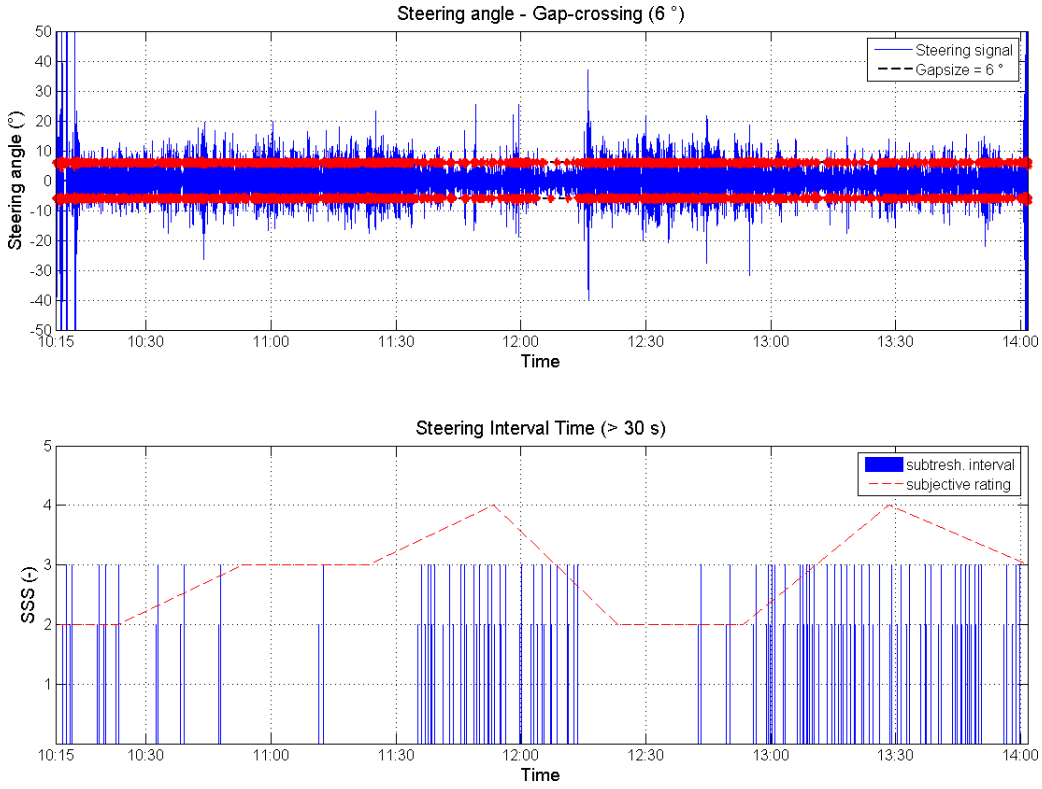

Figure 25: Steering interval time

In the upper part of figure 25 the steering signal is plotted with a gapsize of 6 degrees. The lower part of the figure depicts the steering interval time. Here the start and the end point of the time intervals with an exceeding subthreshold interval are displayed. For the sake of easier discrimination, the start point has a height of 2 and the end point has a height of 3, for each subthreshold interval.

The steering interval time was calculated with a gapsize of 6 degrees with a subthreshold interval of at least 30 seconds. The amount of intervals, in which the subthreshold interval was exceeded, rises in areas with an increasing SSS-rating.

Case 1: Steering Wheel Reversal Rate and Steering Interval Time

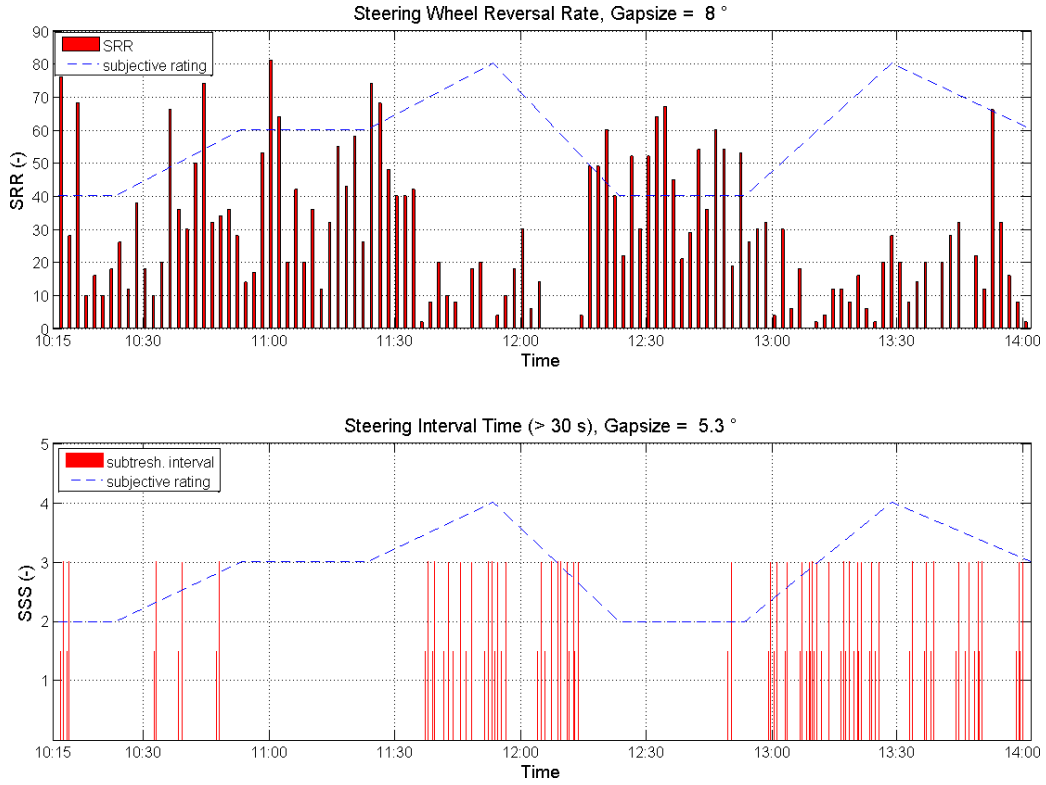

Figure 26: Combined steering wheel reversal rate and steering interval time

In figure 26 the steering wheel reversal rate is combined with the steering interval time. Due to the fact that the SRR and the SIT have a certain relation, cause if the SRR decreases the probabilty of rising time intervals with an exceeding of the non operating time increases. Therefore a connected analysis with the SRR and the SIT was executed. For this the specified gap size for the SRR analysis was reduced by $\frac{2}{3}$ for the analysis of the SIT. With this specification, the identification of reduced attention levels of the driver, through the steering behaviour, can be improved. So, if the SRR is decreasing it is possible to look at exceeding steering intervals at the same point in time. With this concept, areas where the steering angle is close to the gapsize, but does not overstep the gap size can be detected and excluded, if the SIT has no exceedings at this point in time. Such incidents appear in figure 25 e.g. around 11:05 to 11:15, as there the SRR is decreasing, but the SIT shows no exceedings of the subthreshold interval.

Case 2: Steering Signal - Spectrogram

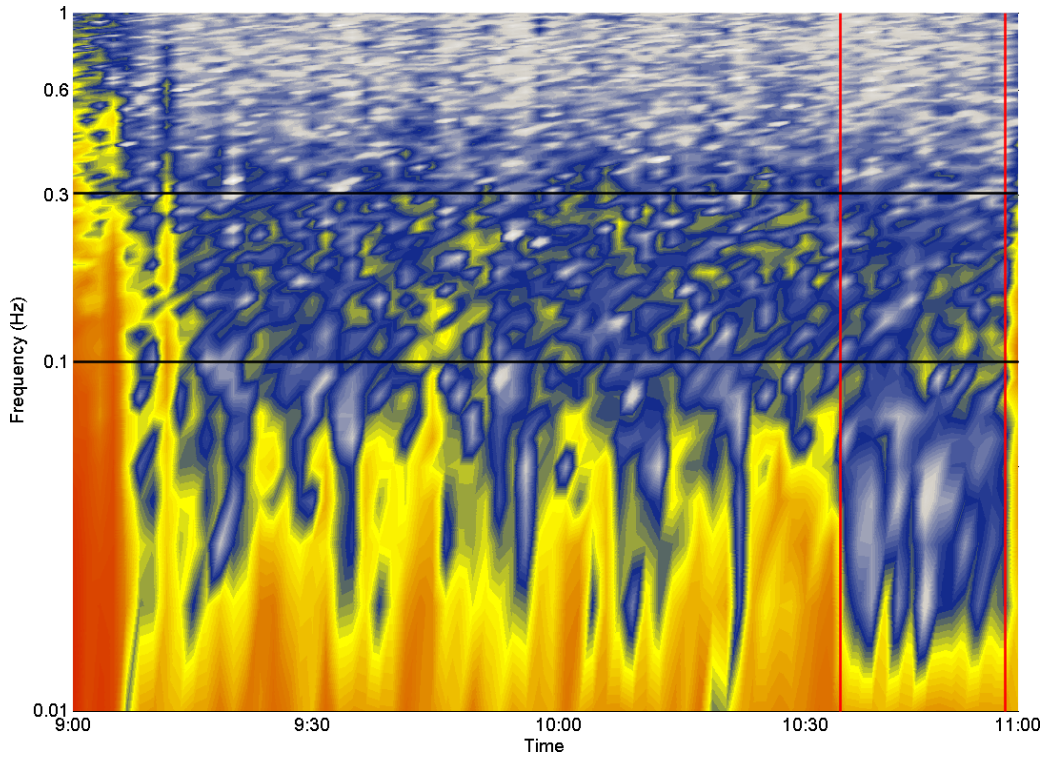

Figure 27: Frequency distribution of the steering behaviour of case 2

Figure 27 shows the steering signal spectrogram of case 2. Here the corrective component (0.3 - 1 Hz) shows almost no activity, except at the beginning of the test drive, where the truck was directed to the motorway. At the time period of increasing fatigue, with ans SSS- rating from '4' to '5' at 10:35 to 11:00, the power of the corrective component diminishes as well as the power of the predictive component. Hence, the cutoff frequency of the steering movements, is decreasing to ≈0.02 Hz, similar to case 1. The rising of the high frequency power at the end of the test ride is explicable by driving the truck to a motorway service area.

Case 2: Steering Wheel Reversal Rate

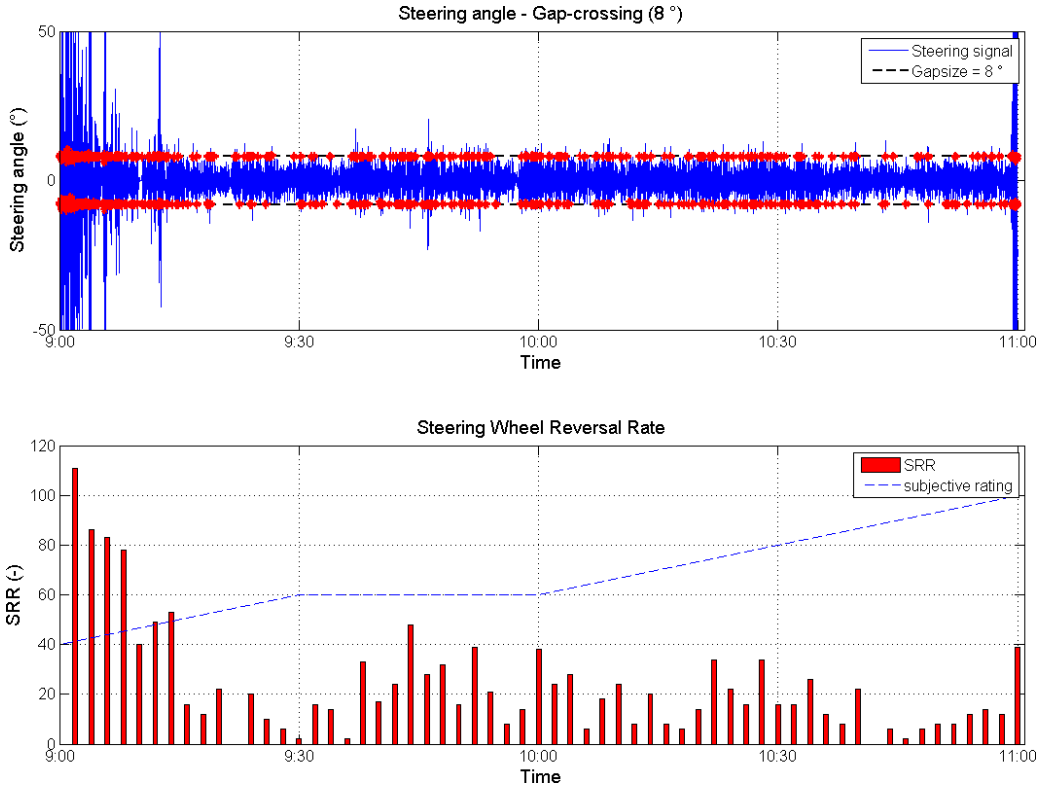

Figure 28: Steering wheel reversal rate

As seen in figure 28 the steering wheel reversal rate decreases continuously, as the SSS-rating increases. The low SRR sequence from 10:35 to 11:00 corresponds with the steering signal spectrogram, also the departure of the motorway to the service area can be detected through the last enlarged SRR value.

Case 2: Steering Interval Time

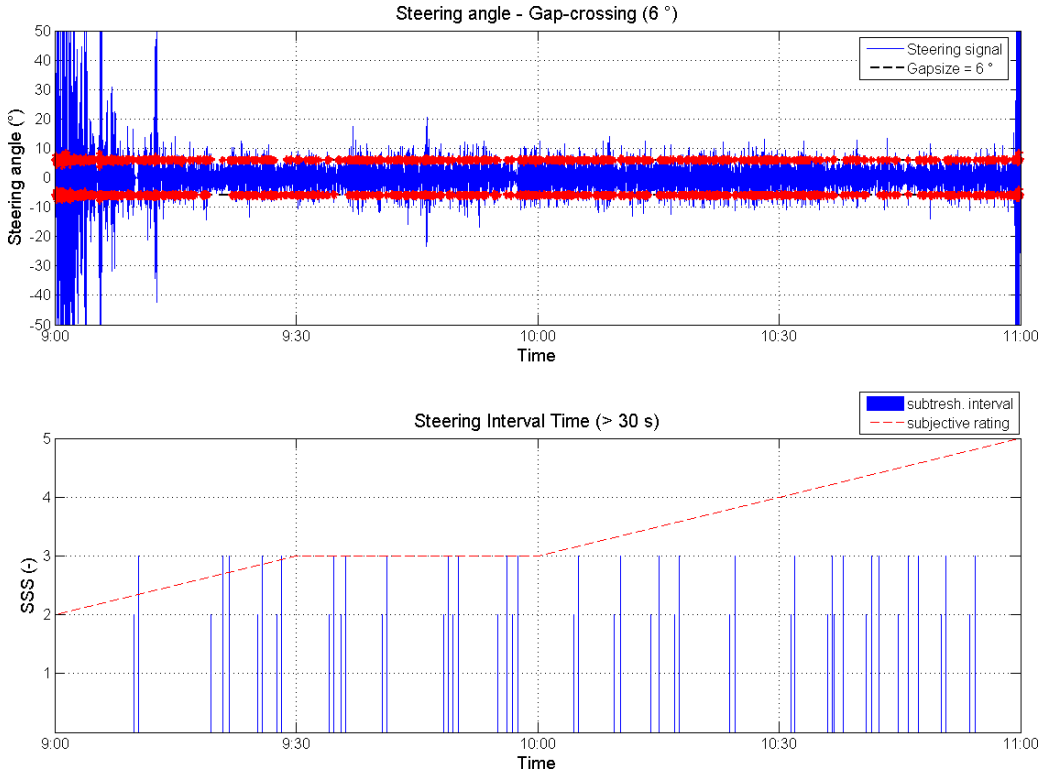

Figure 29: Steering interval time

The steering interval time shows time intervals, in which the specified gap size of 6 degrees was not overstepped for at least 30 seconds. The distribution of these intervals is quite uniform and suggests that subject 2 had an increased fatigue level during the whole test ride. Even though, there is a slight increase of subthreshold interval detectable. This is in agreement with the results of the SRR and the spectrogram.

Case 2: Steering Wheel Reversal Rate and Steering Interval Time

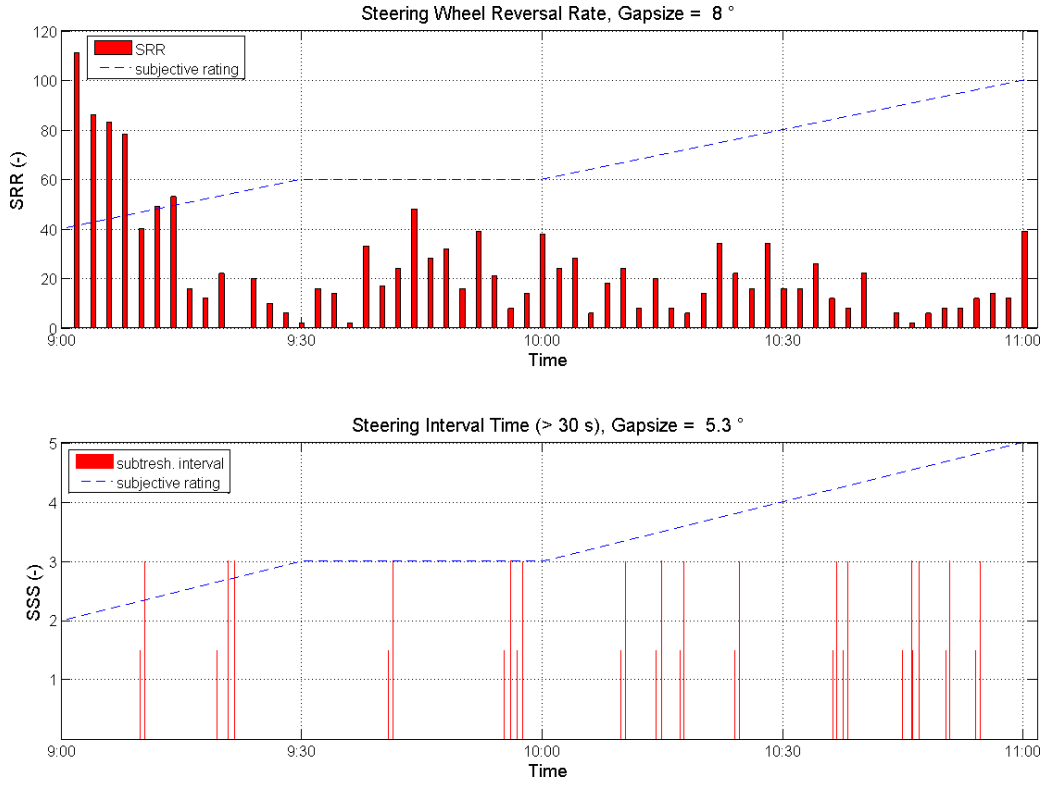

Figure 30: Combined steering wheel reversal rate and steering interval time

The combined analysis of the steering wheel reversal rate and the steering interval time, with the different gap sizes, shows some discrepancies. E.g. at 9:30 the SRR has very low values at a SSS-rating of '2' to '3', but at this point in time no exceeding steering time intervals of $\frac{2}{3}$ gapsize are observable. This means that the steering activity lies somewhere between the two gap sizes. During the last half hour of the test ride, the SRR corresponds quite well with the SIT.

3.1.4 Correlations

A cross correlation between two signals, which are showing satisfying results individually, was executed. Therefore the direct and the indirectly measured values had to show individual

results in order to get according results from the cross correlation. Hence, the cross correlation was only carried out between such signals which showed a cleary visible consistent trend.

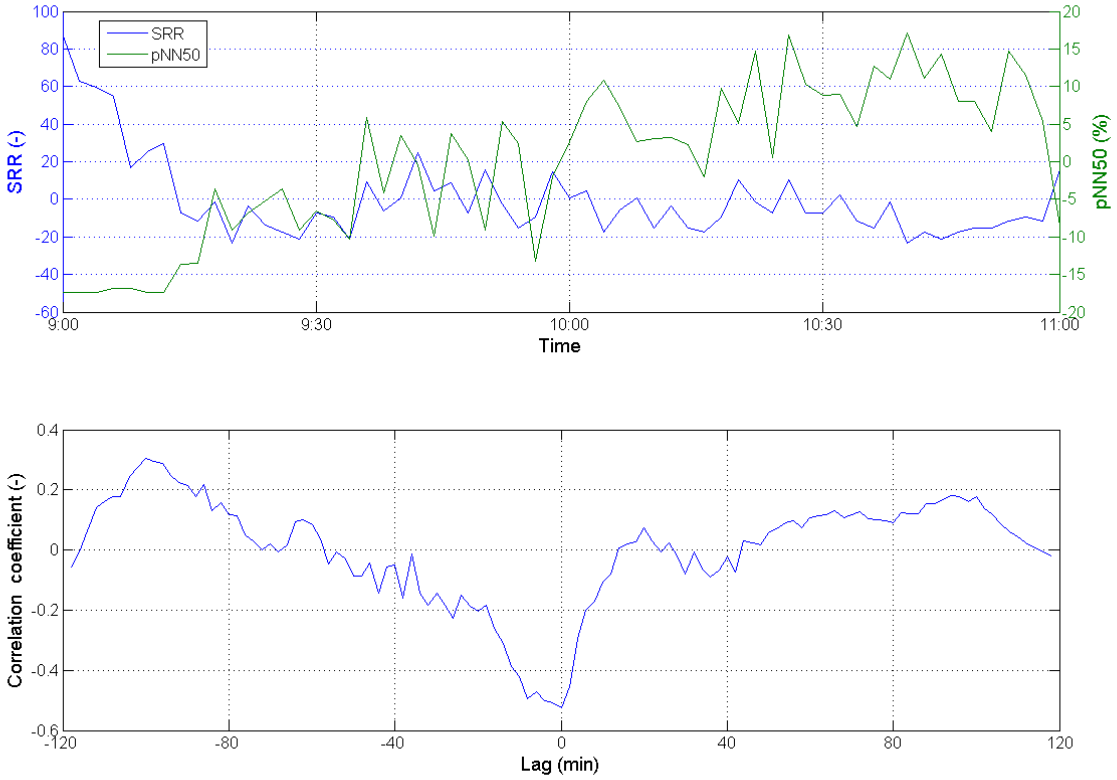

Figure 31: Cross correlation of pNN50 and SRR of case 2

In figure 31 the percentage of RR-Intervals, which varies more than 50ms and the steering interval have a correlation coefficient of ≈ -0.55 at a lag of 0. The positive trend of pNN50 and the negative trend of the SRR (mainly in the second hour) are the reason for that coefficient.

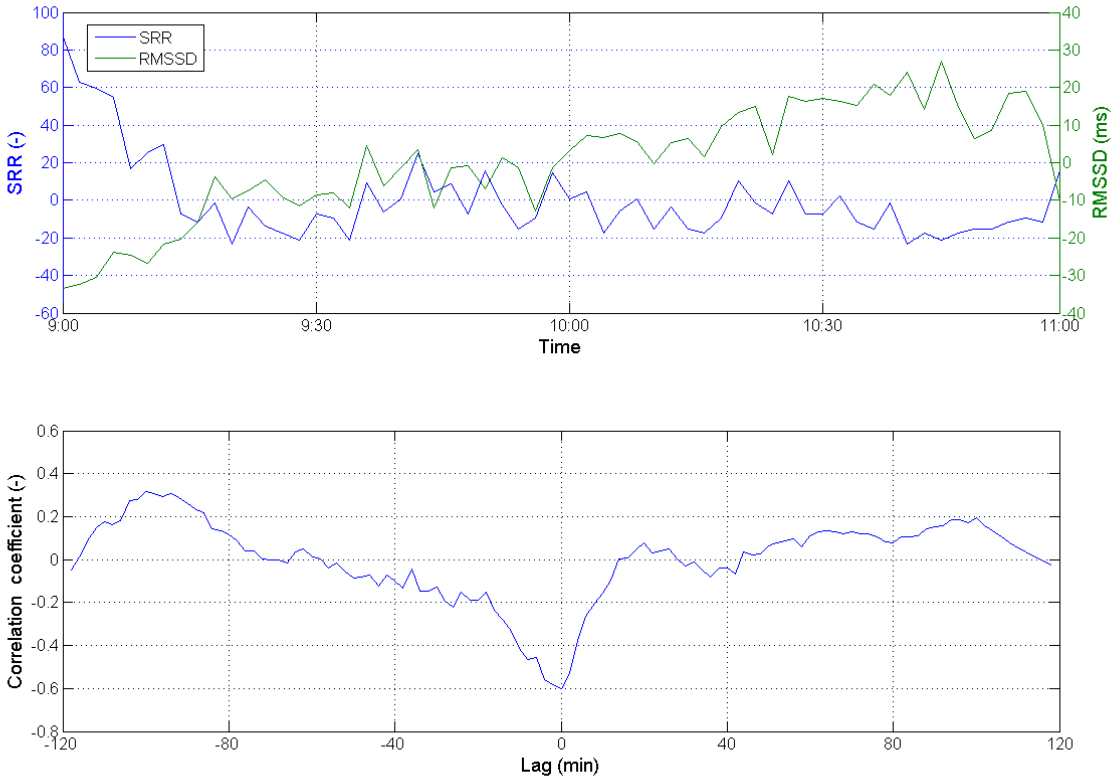

Figure 32: Cross correlation of RMSSD and SRR of case 2

Figure 32 shows similar trends as figure 31, which lead to a correlation coefficient, at a lag of 0, of ≈ -0.6.

3.2 Reaction time study

3.2.1 Main component analysis

RMSSD analysis

Cross correlations between the logged values of the 12 subjects were executed. As HRV index the RMSSD value was used. The results of these correlations are listed in table 11.

Subject	Corr (RT, SSS)	Corr (RMSSD, RT)	Corr (RMSSD, SSS)	Mean
1	0.80	0.27	0.55	0.54
2	0.86	-0.06	0.16	0.32
3	0.50	0.62	0.89	0.67
4	0.84	0.85	0.93	0.87
5	0.86	0.62	0.78	0.75
6	0.11	0.03	0.85	0.33
7	0.73	0.33	0.24	0.43
8	0.81	-0.78	-0.66	-0.21
9	-0.05	0.27	0.06	0.09
10	0.73	0.69	0.53	0.65
11	0.60	0.85	0.69	0.71
12	0.88	0.89	0.88	0.88

Table 11: RMSSD, RT and SSS correlations

To illustrate the results of the 12 subjects in a meaningful and concise way, 3 representative results were selected for plotting. These are the results with the highest (Subject 12) and the lowest correlation (Subject 8), and the correlation closest to the mean of all the subjects (Subject 1).

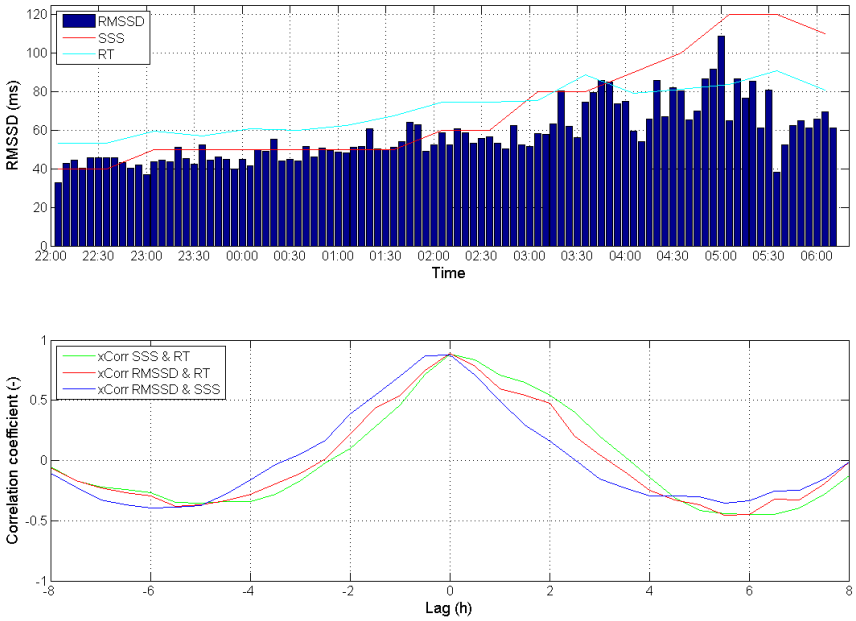

Figure 33: Correlation results of subject 12

Figure 33 shows a continuous increase of the RMSSD, which correlates well with the RT and the SSS. Also the correlation between the RT and the SSS results in a corresponding coefficient. Also the fact, that the maximum correlation appears at a lag of zero at all 3 signals, shows that the RMSSD is a good delay-free indicator of drowsiness for subject 12.

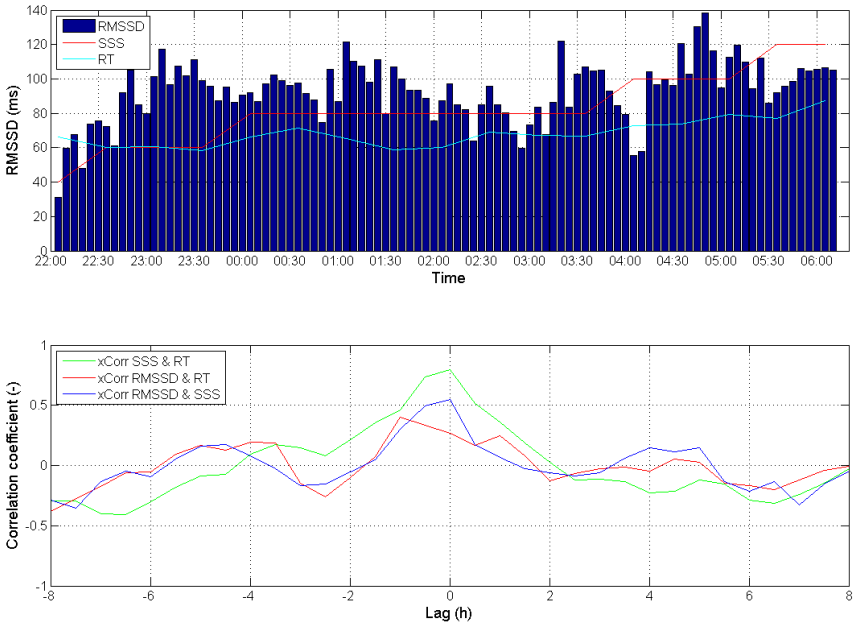

Figure 34: Correlation results of subject 1

In figure 34 the highest correlation appears between the RT and the SSS. The RMSSD has a higher correlation with the SSS than with the RT. The correlation of the RMSSD and the RT shows a better result at a lag of $\approx -1h$, which results from a decrasing RT in the first hour. This can indicate a training effect at the begin of the testing, when the drowsiness is at a low level and has not much influence on the RT.

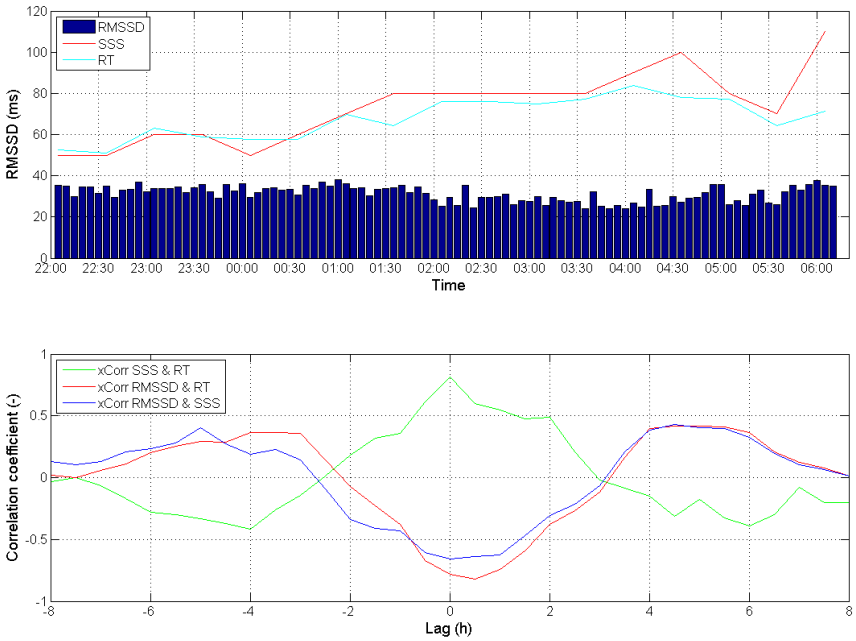

Figure 35: Correlation results of subject 8

Figure 35 shows the subject with the lowest mean of the correlations. This results from the slight decrease of the RMSSD, beginning at $\approx$ 2am, combined with an increase of the RT and the SSS.

pNN50 analysis

Also the pNN50 value of the HRV was correlated with the RT and the SSS of each subject. The results of this correlations are listed in table 12. Row 1 contains the same values as in table 11, cause just the HRV index changed from RMSSD to pNN50 and the RT and the SSS are the same.

Equally to the analysis of the correlations with the RMSSD, the correlation of the subjects with the highest, the lowest and the correlation closest to the average of the 12 subjects is plotted.

Subject	Corr (RT, SSS)	Corr (pNN50, RT)	Corr (pNN50, SSS)	Mean
1	0.80	0.02	0.41	0.41
2	0.86	-0.10	0.11	0.29
3	0.50	0.56	0.87	0.64
4	0.84	0.80	0.90	0.85
5	0.86	0.70	0.76	0.77
6	0.11	0.08	0.82	0.34
7	0.73	0.22	0.09	0.35
8	0.81	-0.67	-0.57	-0.14
9	-0.05	0.25	0.21	0.13
10	0.73	0.72	0.62	0.69
11	0.60	0.86	0.76	0.74
12	0.88	0.88	0.87	0.88

Table 12: pNN50, RT and SSS correlations

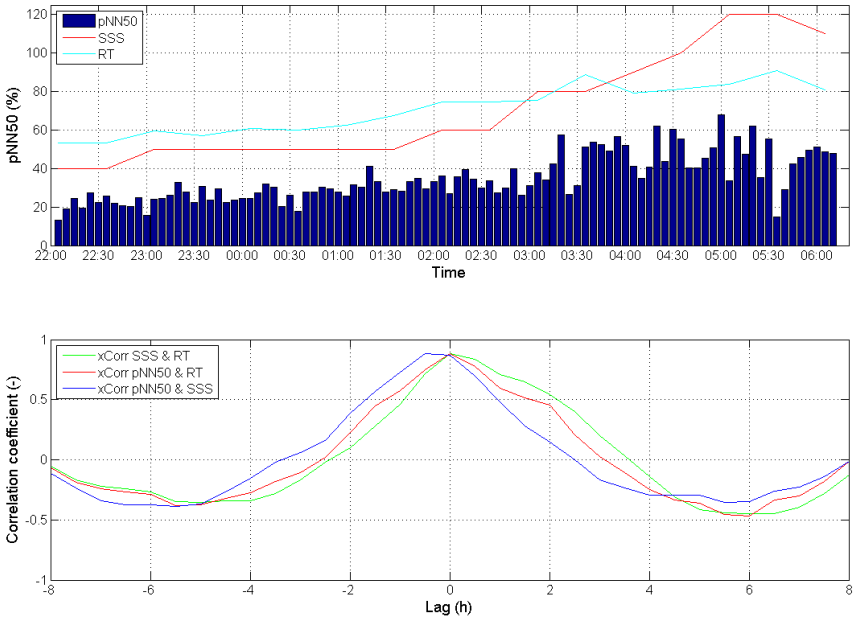

Figure 36: Correlation results of subject 12

Similiar to the results of the RMSSD correlations, the pNN50 correlations have a similar distribution and lead to the highest mean of the correlations.

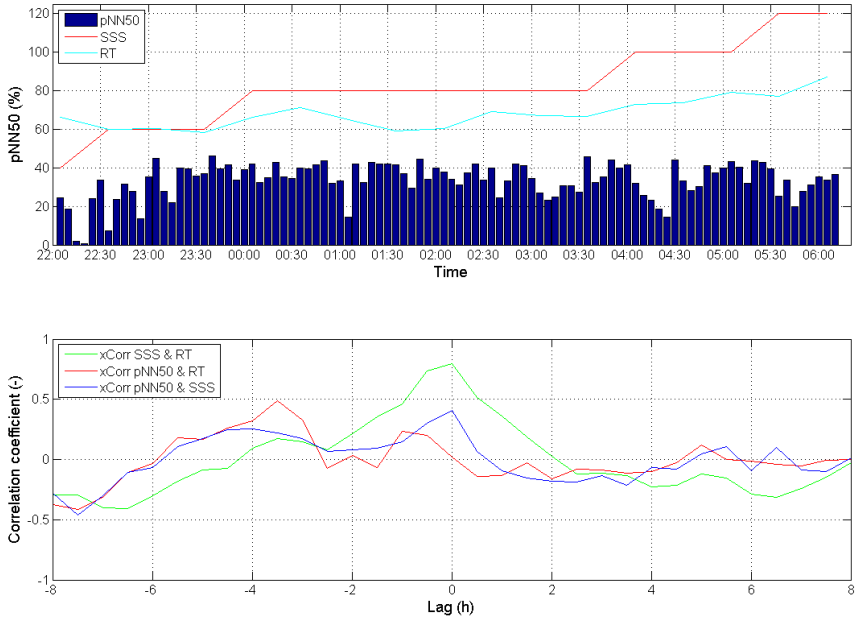

Figure 37: Correlation results of subject 1

While the pNN50 stays comparatively constant, except in the first hour, the RT and the SSS rises through the entire testing time. The correlation between the pNN50 and the RT at a lag of 0 is almost 0. The fact that the increase of the RT at $\approx$ 3am, does not correspond with the pNN50, leads to the r_{Corr} of ≈ 0.5 at a lag of $\approx -3.5h$.

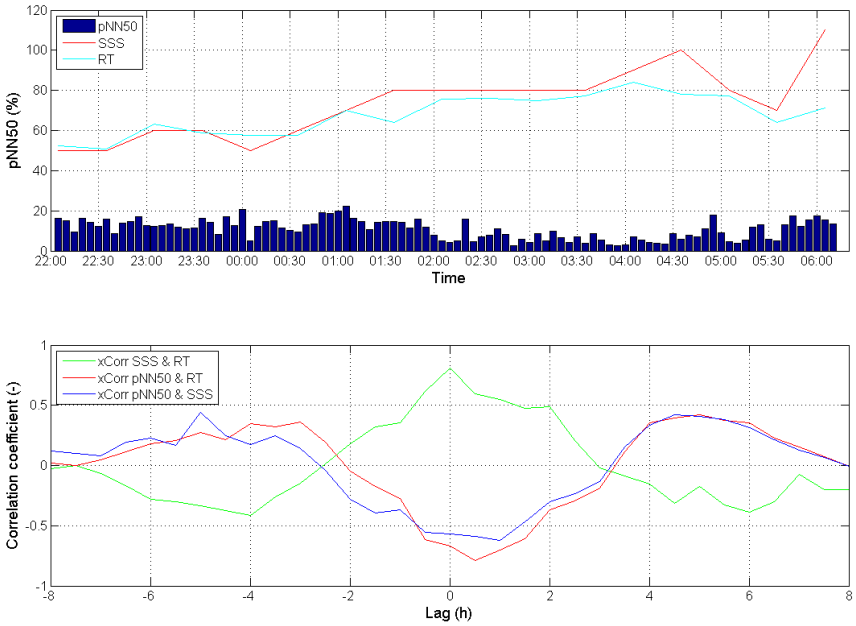

Figure 38: Correlation results of subject 8

LF/HF analysis

The correlations of the LF/HF ratio with the RT and the SSS are listed in table 13. The correlation of the RT and the SSS are not listed in this table, because they are already displayed in table 11 and 12.

Subject	Corr (LF/HF, SSS)		Corr (LF/HF, RT)	
	Parametric	Nonparametric	Parametric	Nonparametric
1	0.09	0.02	0.38	0.21
2	-0.33	-0.32	-0.17	-0.26
3	-0.54	-0.45	-0.06	0.00
4	-0.06	-0.30	0.19	-0.02
5	-0.38	-0.42	-0.35	-0.34
6	-0.27	-0.38	0.46	0.43
7	-0.20	-0.46	-0.21	-0.36
8	0.31	0.19	0.24	0.15
9	-0.21	0.02	-0.53	-0.53
10	-0.20	-0.24	0.13	-0.06
11	-0.44	-0.25	-0.73	-0.63
12	0.70	0.31	0.70	0.27

Table 13: LF/HF, RT and SSS correlations

As seen, the frequency domain of the HRV has no relevant information about the drowsiness level of the subjects. Only Subject 12 shows two noticeable correlations, by using the the parametric method for calculating the PSD.

3.2.2 Cluster analysis - K mean algorithmus

For this analysis only the time domain indices of the HRV were considered, due the better correlation results as seen in the previous chapter.

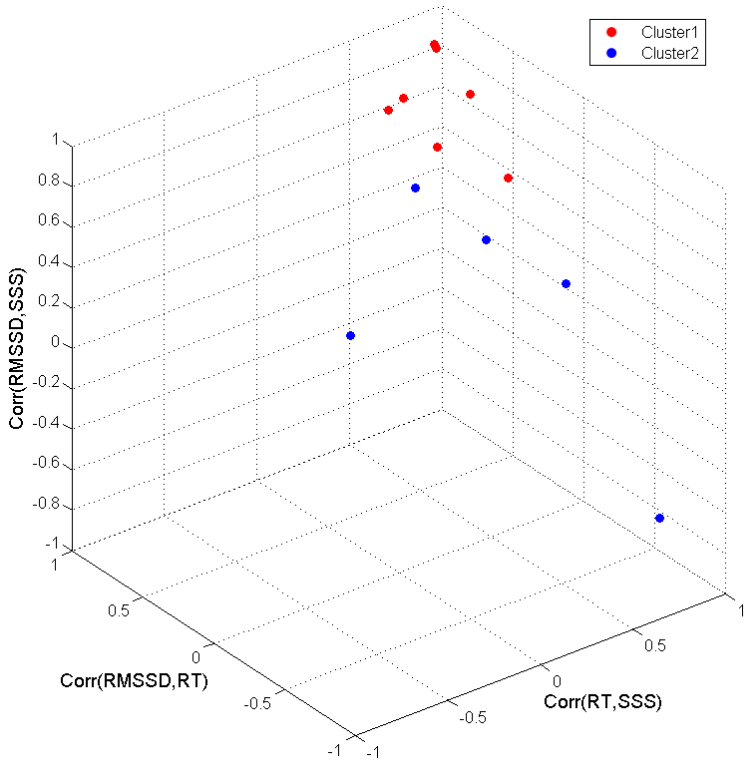

Figure 39: Cluster of RMSSD correlations

Cluster	Subject
1	1,3,4,5,10,11,12
2	2,6,7,8,9

Table 14: Segmentation of the subjects into 2 clusters, due the RMSSD

As seen in figure 39 and table 14, cluster 1 includes 7 subjects and cluster 2 includes 5 subjects. Subject 1 has the lowest mean r_{Corr} with 0.54 of Cluster 1 and Subject 7 has the highest mean r_{Corr} with 0.43 of Cluster 2. These two Subjects (1 and 7) build the gap to classifiy the whole group into responders (Cluster 1) and into non-responders (Cluster 2) of using the RMSSD as indicator for drowsiness.

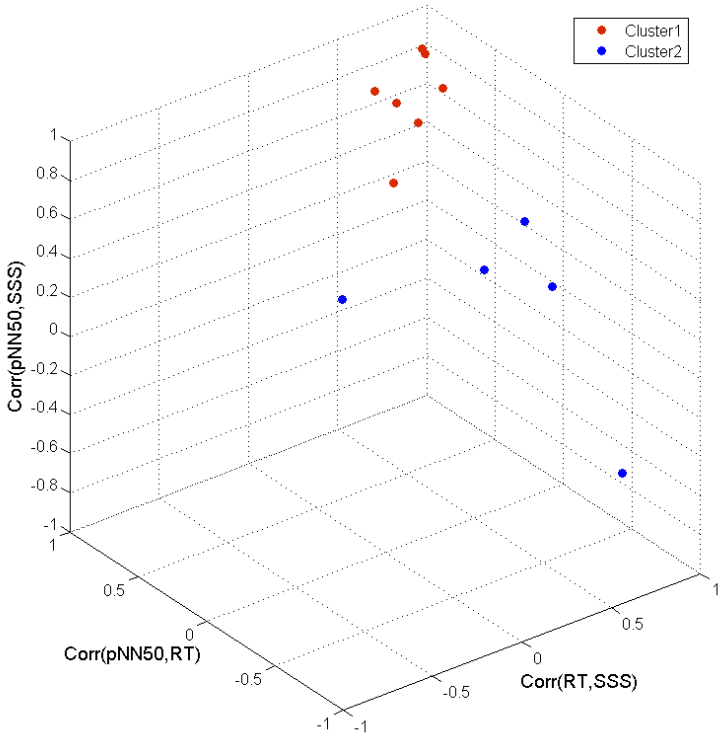

Figure 40: Cluter of pNN50 correlations

Cluster	Subject
1	3,4,5,6,10,11,12
2	1,2,7,8,9

Table 15: Segmentation of the subjects into 2 clusters, due the pNN50

The cluster analysis based on the correlations of the pNN50, as seen in figure 40 and table 15, shows an almost similar result as the correlations of the RMSSD. Two Subjects (1 and 6) switched the clusters in comparison to the RMSSD correlations. Altough subject 6 has a lower mean r_{Corr} than subject 1, it is assigned to cluster 1, which include the responers. This happened because the euclidean difference of subject 6 to the centroid of cluster 1 is shorter than to cluster 2. For subject 1 the contrary is true.

3.2.3 Cluster analysis - Dendrogram

The first dendrogram was computed with the correlations between RMSSD and RT and the SSS for two input parameters. The r_{Corr} between the RT and the SSS was the third input parameter.

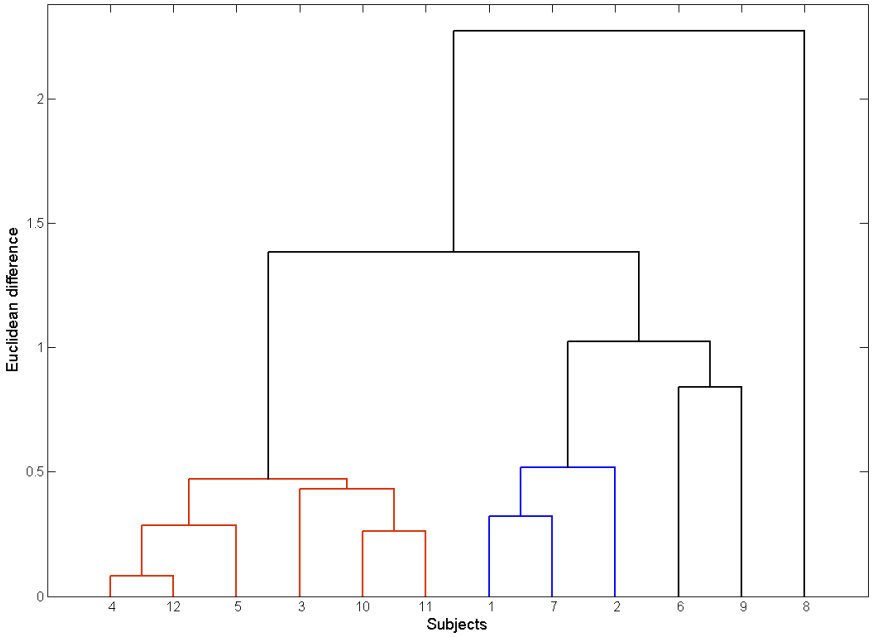

Figure 41: Dendrogram of the RMSSD correlations

Group		Euclidean difference
Joint 1	Joint 2	
4	12	0.08
10	11	0.26
5	13	0.29
1	7	0.32
3	14	0.43
15	17	0.47
2	16	0.52
6	9	0.84
19	20	1.02
18	21	1.38
8	22	2.27

Table 16: Aggregation of the RMSSD correlations, due the euclidean difference

The dendrogram in figure 41 illustrates that there are two clusters (red and blue) which include subjects with a response characteristic. The red cluster can be classified as group with considerable responders and the blue cluster as group with normal reponders. The third cluster (black) includes subjects, which showing no response for RMSSD as drowsiness indicator. It is easy to see that subject 8 shows the most dissimilarities to the other subjects because it is grouped as last one, together with subject 6 and 9. The red and blue clusters are characterized through groupings with a short distance (≤ 0.52), which suggest a high similarity between these subjects.

The second dendrogram was computed with the correlations of the pNN50 with the RT and the SSS, and the correlation of the RT and the SSS.

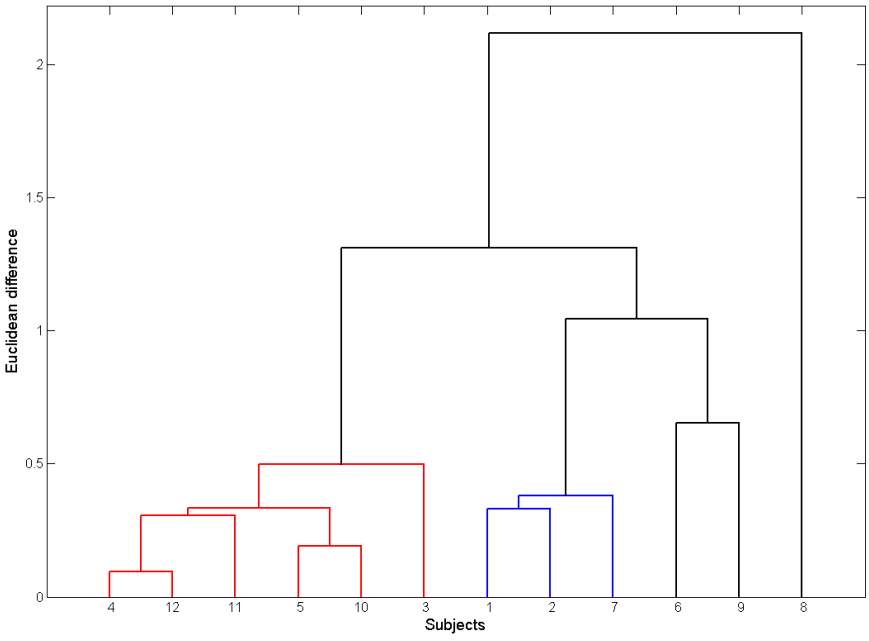

Figure 42: Dendrogram of pNN50 correlations

The dendrogram shown in figure 42, in which the pNN50 is used as HRV index, and the dendrogram where the RMSSD is used as HRV index (Figure 41) are showing practically the same result. A small difference is the distribution of the subjects within the computed clusters. Also the aggregation stays the same, leaving the subjects 6,8 and 9 in a group of definite non-responders and the rest are basically clustered in a responders group. These responders are

Group		Euclidean difference
Joint 1	Joint 2	
4	12	0.09
5	10	0.19
11	13	0.30
1	2	0.33
14	15	0.33
7	16	0.38
3	17	0.50
6	9	0.65
18	20	1.05
19	21	1.31
8	22	2.12

Table 17: Aggregation of the pNN50 correlations, due the euclidean difference

further divided into the red and the blue cluster, where the red cluster includes the subjects with a more considerable correspondence for the pNN50 as drowsiness indicator than the blue cluster.

4 Discussion

The findings in the driving study revealed a consistency between the direct and indirect approach from subject 2 and a discrepance from subject 1. More precisely, the time domain indices of the HRV corresponded well with time domain indices of the steering signal during an increasing SSS-rating, on a test drive of subject 2. In contrast an increased SSS-rating of subject 1 did not correlate with the HRV inidices in the time domain, however the indices of the steering signal corresponded well with the subjective rating. The frequency domain indices of the HRV showed no clear relationship with the steering signal and/or the subjective drowsiness rating. The influence of the respiratory sinus arrhythmia on the frequency distribution of the HRV, as described in chapter 2.2.2, is probably a major reason for the lack of correlation. To obtain clear frequency components reflecting to the physiological state, the subjects should probably breathe with a given rhythm (controlled respiration) as done in [9].

The analysis of the steering signal itself, correlated with the subjective drowsiness rating for both of the subjects according to the , i.e. the steering wheel reversal rate and the steering interval time, showed results corresponding to [26, 27]. In contrast it appeared not always possible to predict an increased fatigue from HRV. Unfortunately, the correlation between the SSS-rating and the indices of the steering signal cannot be seen as an entirely reliable indicator for drowsiness. Because if the steering signal is indicating drowsiness, it is also possible that the driver took the hand off the steering wheel for a certain amount of time. Nevertheless the steering signal reflects decreased attention levels, which can be initiated by many factors, like boredom, be lost in thoughts or general distraction.

The results of the reaction time study lead to the conclusion that the subdivided can be specified into a group of responders and into a group of non- responders. The k-mean clustering revealed 7 responders and 5 non-responders. The dendrogramm analysis showed a similar result by grouping the 12 subjects into 3 clusters. Thus the subjects can be specified more precisely, into a cluster of considerable responders, normal responders and non-responders. The cluster with the considerable responders includes 6 subjects, followed by 3 subjects each, in the normal responders and non-responders cluster. The 6 subjects included in the first cluster from the

dendrogram analysis are all in the responders-cluster of the k-means analysis. The 7^th subject from the responders- cluster of the k- mean analysis is not the same in the pNN50 and in the RMSSD correlations, which are the input parameters for the clustering. According to the pNN50 input parameters, the 7^th subject belongs to the normal responders and according to the RMSSD input parameters, the 7^th subject belongs to the non-responders cluster. Hence there is a total correspondence in the responders group and an almost total correspondence in the non-responders group between the k- mean analysis and the cluster analysis.

Interestingly some non-responders cluster, regularly exercise physically (running marathon, rock climbing), play music (drums), or train there reaction velocity by playing computer games. The frequency domain of the HRV showed also no correspondence to increasing drowsiness. The fact that [17] statet an increasing LF to HF ratio during long truck driving work, can be tracked back, that they calculated the mean of this ratio in intervals of 4 hours over 24 hours. In this work the LF/HF ratio was calculated from 5 minutes intervals, according to the time domain indices of the HRV. The long term changes, as calculated in [17], have no relevance in this work, because the comparison requires a much higher time resolution with the other indicators (steering signal, reaction time, subjective rating).

With the information obtained from the reaction time study, the results of the driving study can be better interpreted. The two subjects involved in the driving study, may have different response characteristics. It can be suspected that subject 2 lies in the responder cluster and subject 1 in the non-responder cluster. Unfortunately the two test subjects from the driving study, are not available anymore for the attendance to a subsequent reaction time study. But with the results from the test rides, the possibility of this classification is given.

The purpose of this work, to analyse indicators for the assessment of drowsiness of truck drivers, was achieved, in order to obtain some significant and important findings and some drawbacks. The first part of the work, were the driving study was analyzed, led to the awareness that increased fatigue was observable through the HRV in only one of the two subjects. The observable changes in the steering signal indices, during increasing subjective drowsiness ratings, led to the conlusion, that a decreased attention level can be detected through the steering

behaviour.

The second part of the work, were 12 subjects participated in a reaction time study during sleep deprivation, revealed some additional and significant findings. The information, that not everybodies HRV shows a response during increasing fatigue, and the according clustering into groups with responders and non-responders, is an important step. The important content of this information, is the fact, that truck drivers involved in continuative studies, have to be checked, whether they are responders or non- responders, for using the HRV as fatigue indicator.

For further research, as already mentioned, it is important to verify the response characteristics of the subjects, according to the findings in the reaction time study. Subjects, which are considerable responders, should be taken for doing further test rides, in order to get correct and useful results from the HRV analysis. Furthermore, the number of subjects should be higher and consist of professional truck drivers. The fact that non-professional drivers are easily overstrained by driving a truck with an overall weight of more than 7.5 tons, can tamper the results. Also the number of trucks should be increased in further studies, in order to compare different trucks and their specific influence of drowsiness on the driver.

References

[1] Claudia Evers. Unterschätzte Risikofaktoren – Übermüdung und Ablenkung als Ursachen für schwere LKW Unfälle. In *Bundesanstalt für Straßenwesen: Sicherheit von Nutzfahrzeugen*, 2008.

[2] Ansakorpi H. *Cardiovascular regulation in epilepsy with emphasis on the interictal state.* PhD thesis, University of Oulu, Finland, 2003.

[3] Kobayashi H, Ishibashi K, et al. Heart rate variability: An index for monitoring and analyzing human autonomic activities. *APPLIED HUMAN SCIENCE - Journal of Physiological Anthropology*, 18:53–59, 1999.

[4] Task Force of the European Society of Cardiology the North American Society of Pacing Electrophysiology. Heart rate variability: Standards of measurement, physiological interpretation, and clinical use. *Circulation*, 93:1043–1065, 1996.

[5] Hick C. *Intensivkurs Physiologie.* Elsevier, 2006.

[6] Becker DE. Fundamentals of electrocardiography interpretation. *American Dental Society of Anesthesiology*, 53:53–64, 2006.

[7] Lahiri MK, Kannankeril PJ, et al. Assessment of autonomic function in cardiovascular disease: Physiological basis and prognostic implications. *Journal of the American College of Cardiology*, 51:1725–1733, 2008.

[8] Kurtz F. *Induktionsmechanismen von paroxysmalem Vorhofflimmern: Charakterisierung von Onset- Szenarien und die Rolle des autonomen Tonus.* PhD thesis, Universität zu Lübeck, 2009.

[9] Pagani M, Lombardi F, et al. Power spectral analysis of heart rate and arterial pressure variabilities as a marker of sympatho-vagal interaction in man and conscious dog. *American Heart Association*, 59:178–193, 1986.

[10] Malliani A, Lombardi F, et al. Power spectrum analysis of heart rate variability: a tool to explore neural regulatory mechanisms. *British Heart Journal*, 71:1–2, 1994.

[11] Goldberger JJ. Sympathovagal balance: how should we measure it? *The American Journal of Physiology - Heart and Circulatory Physiology*, 276:1273–1280, 1999.

[12] Malliani A, Pagani M, et al. Cardiovascular neural regulation explored in the frequency domain. *Journal of the American Heart Association*, 84:482–492, 1991.

[13] Opthof T and Coronel R. The normal range and determinants of the intrinsic heart rate in man. *Cardiovascular Research*, 45:175–176, 2000.

[14] Robertson D and Johnson GA. Comparative assessment of stimuli that release neuronal and adrenomedullary catecholamines in man. *American Heart Association*, 59:637–643, 1979.

[15] Lin CT, Wu RC, et al. EEG-based drowsiness estimation for safety driving using independent component analysis. *IEEE Transactions on Circuits and Systems*, 52 No. 12: 2726–2738, 2005.

[16] Sommer D and Golz M. Evaluation of perclos based current fatigue monitoring technologies. In *32nd Annual International Conference of the IEEE EMBS*, 2010.

[17] Sato S, Taoda K, et al. Heart rate variability during long truck driving work. *Journal of Human Ergology*, 30:235–240, 2001.

[18] Yao KP, Lin WH, et al. Real-time vision-based driver drowsiness/fatigue detection system. *(n.d.)*, 2010.

[19] Nasoz F, Lisetti CL, et al. Affectively intelligent and adaptive car interfaces. *Information Sciences*, 180:3817–3836, 2010.

[20] Zhe M and Deqi H. Analysis of steering angle under driving fatigue. In *Second International Workshop on Education Technology and Computer Science*, 2010.

[21] Tobias Altmüller. *Driver Monitoring and Drowsiness Detection by Steering Signal Analysis*. PhD thesis, Universität der Bundeswehr München, 2007.

[22] Hefner R, Edwards D, et al. Operator fatigue estimation using heart rate measures. In *PROCEEDINGS of the Fifth International Driving Symposium on Human Factors in Driver Assessment, Training and Vehicle Design*, 2009.

[23] Shinar Z, Akselrod S, et al. Autonomic changes during wake–sleep transition: A heart rate variability based approach. *Autonomic Neuroscience: Basic and Clinical*, 130:17–27, 2006.

[24] Thayer JF. Heart rate variability: A neurovisceral integration model. *Journal of Affective Disorders*, 2009.

[25] Kay S and Marple SL. Spectrum analysis-a modern perspective. *Proceedings of the IEEE*, 69:1380 – 1419, 1981.

[26] King DJ, Mumford DK, et al. An algorithm for detecting heavy-truck driver fatigue from steering wheel motion. *MacInnis Engineering Associates Ltd.*, US:17–38, 1996.

[27] Fukuda J, Akutsu E, et al. An estimation of driver's drowsiness level using interval of steering adjustment for lane keeping. *Society of Automotive Engineers of Japan*, 94:197–199, 1995.

[28] Reif K and Dietsche KH. *Kraftfahrtechnisches Taschenbuch*. Robert Bosch Gmbh, 2011.

Appendix A

Einwilligungserklärung zur Studie:
"Ermittlung des Reaktionsvermögens bei steigender Müdigkeit"

Ich, _____, geboren am _____,
nehme am _____ freiwillig an der Studie "Ermittlung des Reaktionsvermögens bei steigender Müdigkeit" teil. Ich wurde über den genauen Ablauf und über mögliche Risiken der Studie aufgeklärt. Des Weiteren ist es mir jederzeit und grundlos möglich, die Teilnahme an der Studie abzubrechen.

Ich erfülle eine Nacht vor der Studiendurchführung mein normales und übliches Schlafpensum und übe am Tag der Studiendurchführung keine extremen physischen Anstrengungen aus.

Auch nehme ich am Tag der Studiendurchführung keine koffeinhaltigen oder sonstige aufputschende Substanzen zu mir.

Außerdem stehe ich, in einem Zeitraum von mindestens 2 Wochen vor der Studiendurchführung, unter keiner medikamentösen Behandlung.

Ort, Datum	Unterschrift Teilnehmer	Unterschrift Studienleiter

ACKNOWLEDGEMENTS

The author would like to acknowledge the financial support of the "COMET K2 - Competence Centres for Excellent Technologies Programme" of the Austrian Federal Ministry for Transport, Innovation and Technology (BMVIT), the Austrian Federal Ministry of Economy, Family and Youth (BMWFJ), the Austrian Research Promotion Agency (FFG), the Province of Styria and the Styrian Business Promotion Agency (SFG).

I would furthermore like to express our thanks to our supporting industrial and scientific project partners, namely "AVL List Gmbh, Gesellschaft für Industrieforschung mbH (GIF), Institute of Automotive Engineering" and to the Graz University of Technology.